

Scalable Label Distribution Learning for Multi-Label Classification

Xingyu Zhao, Yuexuan An, Lei Qi, Xin Geng

School of Computer Science and Engineering, Southeast University, Nanjing 211189, China
Key Laboratory of New Generation Artificial Intelligence Technology and Its Interdisciplinary Applications (Southeast University), Ministry of Education, China
Email: {xyzhao, yx_an, qilei, xgeng}@seu.edu.cn

Abstract—Multi-label classification (MLC) refers to the problem of tagging a given instance with a set of relevant labels. Most existing MLC methods are based on the assumption that the correlation of two labels in each label pair is symmetric, which is violated in many real-world scenarios. Moreover, most existing methods design learning processes associated with the number of labels, which makes their computational complexity a bottleneck when scaling up to large-scale output space. To tackle these issues, we propose a novel MLC learning method named Scalable Label Distribution Learning (SLDL) for multi-label classification which can describe different labels as distributions in a latent space, where the label correlation is asymmetric and the dimension is independent of the number of labels. Specifically, SLDL first converts labels into continuous distributions within a low-dimensional latent space and leverages the asymmetric metric to establish the correlation between different labels. Then, it learns the mapping from the feature space to the latent space, resulting in the computational complexity is no longer related to the number of labels. Finally, SLDL leverages a nearest-neighbor-based strategy to decode the latent representations and obtain the final predictions. Our extensive experiments illustrate that SLDL can achieve very competitive classification performances with little computational consumption.

Index Terms—Data mining, Multi-label classification, Label distribution learning, Large-scale output space, Label correlation.

I. INTRODUCTION

Learning with ambiguity is a prominent subject within the machine learning community [1]–[4]. Multi-label classification (MLC) emerges as a common approach to address the challenge of label ambiguity [5], [6]. MLC allows instances to be annotated with multiple labels simultaneously, offering a practical solution to the ambiguity problem. In the context of MLC, each class label is treated as a logical indicator, signifying whether the corresponding label is relevant or irrelevant to the instance. Specifically, +1 denotes relevance to the instance, while -1 signifies irrelevance. Such labels, represented by -1 or +1, are commonly referred to as *logical labels* [4], [7]–[9]. Over the years, various MLC techniques have found widespread application across diverse domains, including document classification [10], image recognition [11], video concept detection [12], temporal action detection [13], fraud detection [14], among others.



(a) labels: *sky*, *cloud*, *plant*



(b) labels: *sky*, *plant*

Fig. 1: An illustration of exemplar images and their corresponding labels. The correlation of “*sky*” and “*cloud*” are asymmetric. Specifically, if “*cloud*” appears in an instance, then “*sky*” also appears; And if “*sky*” appears, “*cloud*” may not necessarily appear.

In real-world MLC problems, exploring the correlations among different labels is a crucial research area. Label correlation yields more accurate label information compared to the original logical labels, making it a valuable aspect to enhance the learning capabilities of MLC models. Numerous research efforts aim to uncover label correlation information to enhance the learning capabilities of MLC models, such as classifier chain-based approaches [15]–[17], sequence-based approaches [18], deep embedding approaches [19]–[21], label distribution learning (LDL)-based approaches [22]–[24], etc. Given the importance of effectively mining underlying information from different labels, the exploration of label correlation is widely undertaken in various real-world multi-label tasks [25]–[27].

However, existing MLC methods grapple with two primary challenges. Firstly, a prevalent assumption in many of these methods is that label correlations within each label pair are symmetric, which often does not hold in real-world scenarios. For instance, Fig. 1 illustrates two images which are annotated with labels “*sky*”, “*cloud*”, “*plant*” and “*sky*”, “*plant*”, respectively. Notably, the correlation between “*sky*” and “*cloud*” is asymmetrical. Specifically, if “*cloud*” appears in an instance, “*sky*” also appears; nevertheless, if “*sky*” appears, “*cloud*” may not necessarily be present. Recognizing and accounting for such asymmetric correlations between labels can provide more accurate information for MLC, necessitating a shift away from the assumption of symmetric label correlations [28],

[†] Source code is available at <https://github.com/ailearn-ml/SLDL>.

[29]. Secondly, many existing methods tailor their learning processes based on the number of labels, leading to computational complexities that become bottlenecks when scaling up to large-scale output space MLC tasks. These tasks introduce new computational and statistical challenges, prompting the need for more scalable and efficient MLC methodologies.

To address these challenges, we propose Scalable Label Distribution Learning (SLDL) for multi-label classification. SLDL characterizes distinct labels through latent distributions with asymmetric label correlations which are independent of the number of labels. Specifically, SLDL first transforms labels into continuous distributions within a low-dimensional Gaussian embedding space. To effectively capture the accurate correlation among different labels, it employs an asymmetric metric to establish label correlations in the Gaussian embedding space. Subsequently, it learns a mapping from the feature space to the latent space, where computational complexity is no longer tied to the number of labels. Finally, SLDL utilizes a nearest neighbor-based strategy to decode the latent representations and generate the ultimate predictions. This approach significantly enhances both the scalability and classification performance of the model, offering a promising solution to the computational challenges posed by multi-label classification tasks with large-scale output space.

Our contributions are as follows:

- We introduce Scalable Label Distribution Learning (SLDL) as a scalable and effective solution for multi-label classification tasks with large-scale output space.
- We articulate different labels within a latent low-dimensional Gaussian embedding space and propose an asymmetric metric to effectively capture the accurate correlation among different labels.
- We induce a simple yet effective approach to learn the mapping from the feature space to the latent low-dimensional embedding space, where the computational complexity is no longer related to the number of labels.
- We conduct comprehensive analyses of the proposed SLDL method, demonstrating its superior performance in addressing multi-label classification tasks with large-scale output space both theoretically and practically.

The subsequent sections of the paper are structured as follows. Firstly, Section II provides a concise review and discussion of related work. Secondly, Sections III delve into the technical details and theoretical analysis of Scalable Label Distribution Learning (SLDL). Following this, Section IV presents the results of comparative experiments. Lastly, Section V draws conclusions about SLDL.

II. RELATED WORK

A. Multi-Label Classification

In recent years, the field of multi-label classification (MLC) has witnessed significant attention [30], [31]. Traditional multi-label classification approaches fall into three main categories based on label correlation order: first-order, second-order, and high-order approaches [5]. First-order methods

[32]–[35] treat multi-label classification as independent binary classification tasks, neglecting potential information sharing among labels and overlooking the mutual benefits of knowledge gained from one label for learning other labels. Second-order approaches [36], [37] focus on pairwise label correlations, emphasizing differences between relevant and irrelevant labels without fully leveraging relationships among multiple labels. High-order methods [38]–[42] extend beyond pairwise correlations to consider relationships among label subsets or all class labels, aiming for a more comprehensive label space representation. However, a common limitation is their assumption of equal label importance.

To address this limitation, researchers have explored assigning different weights to labels based on class frequencies. For instance, [43] introduces the distribution-balanced loss to rebalance weights and alleviate the over-suppression of negative labels. An alternative is the use of an asymmetric loss, as seen in [44], employing different γ values to weight positive and negative samples in focal loss [45]. Additionally, [46] combines negative-tolerant regularization (NTR) [43] and class-balanced focal loss (CB) [47] to create a novel loss function called CB-NTR. Balanced softmax [48] transforms the multi-label classification loss into comparisons between relevant and irrelevant label scores to balance label importance. However, these methods rely on manually designed rules and lack the ability to dynamically adjust label importance based on specific instances. Moreover, they often overlook correlations among different labels, which are valuable for accurate predictions and should be fully leveraged.

Regarding large-scale output space multi-label classification tasks, existing approaches can be categorized into four types: 1) One-vs-all, 2) Tree-based, 3) Embedding-based, and 4) Deep learning-based methods. One-vs-all methods [49], [50] employ a separate binary classifier for each label when classifying a new instance. Tree-based methods [34], [51] adopt decision tree principles. Embedding-based approaches [38], [39], [41], [52] aim to reduce the effective number of labels by projecting label vectors into a lower-dimensional space. Deep learning-based methods [53], [54] incorporate the latest deep learning technologies into large-scale output space classification. It should be noticed that most existing multi-label classification methods link the learning process to the number of labels, which seriously affects their scalability. Simultaneously, these methods often neglect to capitalize on asymmetric correlations among different labels, which restricts the performance of classification models.

B. Label Distribution Learning

Label Distribution Learning (LDL) has emerged as a promising paradigm for uncovering correlations among different labels, assigning a label distribution to an instance and directly learning a mapping from instance to label distribution [4], [55], [56]. LDL has demonstrated success in various real-world applications, including facial landmark detection [57], age estimation [58], head pose estimation [59], zero-shot learning [60], and emotion analysis from texts [61]. The field

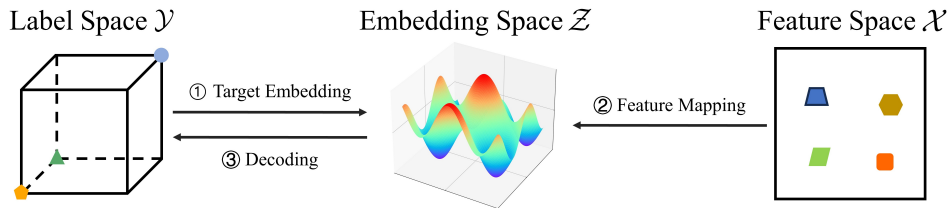


Fig. 2: The schematic diagram of SLDL. The whole process of SLDL can be divided into three parts: (1) target embedding: transform the label vectors into low-dimensional embedding vectors, where the asymmetric label correlations are constructed; (2) feature mapping: learn a mapping function from feature space \mathcal{X} to embedding space \mathcal{Z} , where the computational complexity is no longer related to the number of labels; (3) decoding: map the target embedding vector to the predicted label vector.

has seen the development of specialized LDL algorithms such as SA-IIS and SA-BFGS [4] which integrate the maximum entropy model [62] and K-L divergence using the improved iterative scaling strategy [63] and the BFGS algorithm respectively for optimization. SCE-LDL [64] introduces sparsity constraints into the objective function to enhance the model. Novel ideas have also been incorporated into LDL, including viewing it as a regression problem (LDSVR [65]), using differentiable decision trees (LDL Forests [66]), and developing a deep neural network-based model called Deep LDL [67].

Efforts to exploit label correlations within LDL can be categorized into three main groups: 1) global label correlation, 2) local label correlation, and 3) both global and local label correlations. For global label correlation, methods including EDL [68], LDLLC [69], IncomLDL [70], LALOT [71], and LDLSF [72] adopt various strategies to incorporate label correlations into their optimization objectives. Addressing local label correlation, EDL-LRL [73], GD-LDL-SCL [74], and Adam-LDL-SCL [75] focus on capturing local label correlations within clusters of samples. For both global and local label correlations, LDL-LCLR [76] captures global correlations with a low-rank matrix and updates it on different clusters to explore local label correlation. CLDL [77] leverages the continuous nature of labels to extract high-order correlations among different labels. It is essential to highlight that the computational complexity of LDL is generally higher than traditional learning frameworks, particularly when extending logical labels to label distribution vectors. This complexity significantly increases with a large number of labels, rendering these algorithms impractical. Moreover, existing methods often neglect to leverage asymmetric correlations among different labels, which further limits the performance of the model.

In the next section, we will introduce a novel approach for multi-label classification tasks with large-scale output spaces named Scalable Label Distribution Learning (SLDL). SLDL differs substantially from existing MLC and LDL methods. In SLDL, labels are considered as a continuous distribution in the latent low-dimensional space. Learning in this continuous label distribution space allows for the effective capture of asymmetric label correlations. Moreover, the computational complexity is no longer tied to the number of labels, substantially improving the scalability of the model.

III. THE SLDL METHOD

A. Problem Setting

Firstly, the primary notations employed in this paper are defined as follows. Let $\mathcal{D} = \{(\mathbf{x}_1, \mathbf{y}_1), \dots, (\mathbf{x}_n, \mathbf{y}_n)\}$ represent the given training dataset, where $\mathbf{x}_i \in \mathcal{X} \subset \mathbb{R}^q$ denotes the input feature vector, and $\mathbf{y}_i \in \mathcal{Y} = \{0, 1\}^c$ represents the corresponding label vector, with c denoting the number of possible labels. Define $\mathbf{X} = [\mathbf{x}_1, \dots, \mathbf{x}_n]$ as the data matrix and $\mathbf{Y} = [\mathbf{y}_1, \dots, \mathbf{y}_n]$ as the label matrix. For an instance $\mathbf{x} \in \mathbb{R}^q$, the objective is to train a multi-label classifier $h(\mathbf{x}) : \mathbb{R}^q \rightarrow \{0, 1\}^c$ to predict the proper labels for \mathbf{x} .

B. Overview

In various practical applications, the dimensionality of the output space can be exceedingly high. To handle this challenge, SLDL incorporates the target embedding method, aiming to reduce label dimensionality and mitigate resource requirements during model training. As illustrated in Fig. 2, SLDL first transforms \mathbf{y}_i into an embedding vector $\mathbf{z}_i \in \mathcal{Z} = \mathbb{R}^{\hat{c}}$, where $\hat{c} \ll c$. Subsequently, SLDL learns the mapping from the instance to the low-dimensional embedding vector, denoted as $\mathcal{F} : \mathbf{x}_i \rightarrow \mathbf{z}_i$. During the prediction phase, the output score is decoded from the predicted embedding vector using a nearest neighbor-based strategy. This methodology substantially reduces the resource consumption of the algorithm while effectively exploring the asymmetric correlation among different labels. In the remainder of this section, we will present the implementation of the SLDL method.

C. Asymmetric-Correlational Gaussian Embedding

In SLDL, the extraction of asymmetric correlations is facilitated through the utilization of Gaussian embedding whose capacity offers a flexible and expressive representation of label distributions. To learn a reasonable transition relationship between different labels, we construct a probability transfer matrix. Then, each label is treated as a multivariate Gaussian distribution, and an asymmetric metric is employed to establish the asymmetric correlation between each pair of labels. Through learning in the latent Gaussian embedding space, the continuous distributions that contain the asymmetric correlation among different labels can be effectively learned, which enhances the ability of the model to describe and exploit

Algorithm 1 SLDL: Target Embedding Algorithm

Required: Training dataset: $\mathcal{D} = \{(\mathbf{x}_i, \mathbf{y}_i)\}_{i=1}^N$

Required: Embedding dimensionality: \hat{c}

1: Construct the normalized label correlation matrix \mathbf{A} according to Eqs.(1) and (2)

2: Initialize the parameters of random walk simulation according to Eqs.(3) and (4)

3: Performance the random walk processes and obtain the standardized probability transfer matrix according to Eqs.(5) and (6)

4: Initialize the multivariate Gaussian distribution \mathcal{N} for each label

5: Optimize the latent distribution for each label according to Eq.(7)

6: Obtain the target embedding vectors of training samples according to Eq.(9)

Output: Target embedding matrix \mathbf{Z} of training samples

the nuanced asymmetric correlations inherent in real-world multi-label classification scenarios.

1) *Probability Transfer Matrix Construction:* We first construct a label correlation matrix $\mathbf{A} \in \mathbb{R}^{c \times c}$, in which the corresponding element is 1 if the two labels ever co-exist with each other in any sample:

$$\mathbf{A}_{ij} = \begin{cases} 1, & \text{if the label } i \text{ and } j \text{ ever co-exist,} \\ 0, & \text{otherwise.} \end{cases} \quad (1)$$

For each row, we normalize the label correlation vector:

$$\mathbf{A}_{ij} = \frac{\mathbf{A}_{ij}}{\sum_{l=1}^c \mathbf{A}_{il}}. \quad (2)$$

In order to effectively establish the correlation between different labels, we leverage random walk simulation and aggregate the accumulated values. Denote $\mathbf{P}^{(i)}$ as the probability transfer matrix at the i -th step and $\gamma^{(i)}$ as the discount factor balancing the short-term and long-term transfer probabilities. The parameters of random walk simulation are initialized as

$$\mathbf{P}^{(0)} = \mathbf{A}^{(0)}, \quad (3)$$

$$\gamma^{(0)} = 1. \quad (4)$$

Subsequently, we perform the random walk processes several times and obtain the accumulated probability transfer matrix $\mathbf{P}^{(total)}$:

$$\begin{cases} \mathbf{P}^{(i)} \leftarrow \mathbf{P}^{(i-1)} \mathbf{A}^{(i-1)}, \\ \gamma^{(i)} \leftarrow \gamma^{(i-1)} / 2, \\ \mathbf{P}^{(total)} \leftarrow \mathbf{P}^{(total)} + \gamma^{(i)} \cdot \mathbf{P}^{(i)}. \end{cases} \quad (5)$$

After that, we standardize the accumulated probability transfer matrix and obtain the standardized matrix $\hat{\mathbf{P}}^{(total)}$ which can effectively reflect the probability transfer relation among different labels:

$$\hat{\mathbf{P}}_{ij}^{(total)} = \frac{\mathbf{P}_{ij}^{(total)}}{\sum_{l=1}^c \mathbf{P}_{il}^{(total)}}. \quad (6)$$

2) *Learning Asymmetric-Correlational Gaussian Embedding:* After obtain the standardized probability transfer matrix, we can learn the asymmetric-correlational Gaussian embedding. Specifically, we assume each label as a multivariate Gaussian distribution with a diagonal covariance structure $\mathcal{N}(\boldsymbol{\mu}, \boldsymbol{\sigma}^2 \mathbf{I})$, where \mathbf{I} is the identity matrix. We follow a multi-round optimization to generate reasonable distribution for each label. In each round, we perform the optimization for each label. Concretely, for label i , we consider label i as an anchor, and then rank the remaining labels according to the i -th row in $\hat{\mathbf{P}}^{(total)}$, choosing the j -th label of ranked remaining labels as positive label and the $(j+1)$ -th label as negative label. Then the objective function can be formulated as:

$$\min [\text{KL}(\mathcal{N}_i \parallel \mathcal{N}_j) - \text{KL}(\mathcal{N}_i \parallel \mathcal{N}_{j+1}) + \tau]_+, \quad (7)$$

where

$$\text{KL}(\mathcal{N}_i \parallel \mathcal{N}_j) = -\frac{1}{2} \sum_{k=1}^K \left[\log v_{i,j}^{(k)} - v_{i,j}^{(k)} - \tau_{i,j}^{(k)} + 1 \right], \quad (8)$$

denotes the Kullback-Leibler (KL) divergence which establish asymmetric correlation between $\mathcal{N}(\boldsymbol{\mu}_i, \boldsymbol{\sigma}_i^2 \mathbf{I})$ and $\mathcal{N}(\boldsymbol{\mu}_j, \boldsymbol{\sigma}_j^2 \mathbf{I})$ corresponding to labels i and j respectively, τ is the threshold, $v_{i,j}^{(k)} = \frac{\sigma_i^{(k)2}}{\sigma_j^{(k)2}}$, $\tau_{i,j}^{(k)} = \frac{(\boldsymbol{\mu}_i^{(k)} - \boldsymbol{\mu}_j^{(k)})^2}{\sigma_j^{(k)2}}$, K is the dimension of the latent space and $(\cdot)^{(k)}$ denotes the k -th element. We optimize the objective function for several rounds and obtain the Gaussian embedding for each label. Then, for a specific instance i , we leverage the learned Gaussian embedding and its label vector to obtain its embedding vector:

$$\mathbf{z}_i = \sum_{l=1}^c \mathbf{y}_i^{(l)} \boldsymbol{\mu}_l, \quad (9)$$

where $\mathbf{y}_i^{(l)}$ denotes the l -th element of \mathbf{y}_i . The pseudocode of the target embedding algorithm is given in algorithm 1.

D. Model Training and Prediction

1) *Model Training:* The learning process of the model is to learn a mapping function from the feature space \mathcal{X} to the embedding space \mathcal{Z} . After obtain the embedding vector of each instance, we form the embedding matrix \mathbf{Z} for all instances. Then we optimize the following simple yet effective objective function to obtain the model parameter:

$$\mathcal{L}(\mathbf{W}) = \|\mathbf{Z} - \mathbf{X}\mathbf{W}\|_2^2 + \alpha \|\mathbf{W}\|_2^2, \quad (10)$$

where \mathbf{W} represents the model parameter, α is the balancing factor. We utilize the Limited-memory Broyde-Fletcher-Goldfarb-Shanno (L-BFGS) algorithm [78] to minimize the function $\mathcal{L}(\mathbf{W})$. L-BFGS approximates the inverse Hessian matrix using an iteratively updated matrix instead of storing the full matrix, making it suitable for large-scale optimizations. Consider the second order Taylor series of $\mathcal{L}'(\mathbf{W}) = -\mathcal{L}(\mathbf{W})$ at the current estimate of the parameter $\mathbf{W}^{(t)}$:

$$\begin{aligned} \mathcal{L}'(\mathbf{W}^{(t+1)}) &\approx \mathcal{L}'(\mathbf{W}^{(t)}) + \nabla \mathcal{L}'(\mathbf{W}^{(t+1)})^T \boldsymbol{\Delta} \\ &\quad + \frac{1}{2} \boldsymbol{\Delta}^T \mathcal{H}(\mathbf{W}^{(t)}) \boldsymbol{\Delta}, \end{aligned} \quad (11)$$

Algorithm 2 SLDL: Training Algorithm

Required: Training dataset: $\mathcal{D} = \{(\mathbf{x}_i, \mathbf{y}_i)\}_{i=1}^N$
Required: Target embedding matrix \mathbf{Z} of training samples
1: Normalize \mathbf{x}_* using L2-normalization
2: Initialize the model parameter \mathbf{W}
3: Optimize the model parameter \mathbf{W} according to Eq. (10)
Output: Model parameter \mathbf{W}

Algorithm 3 SLDL: Test Algorithm

Required: Training dataset: $\mathcal{D} = \{(\mathbf{x}_i, \mathbf{y}_i)\}_{i=1}^N$
Required: Target embedding matrix \mathbf{Z} of training samples
Required: testing sample \mathbf{x}_*
Required: number of neighbors for predicting: k
1: Normalize \mathbf{x}_* and \mathbf{x}_* using L2-normalization
2: Calculate the transformed embedding matrix $\hat{\mathbf{Z}}$ according to Eq.(17)
3: Obtain the corresponding target vector in the embedding space $\hat{\mathbf{z}}_*$ for \mathbf{x}_* according to Eq.(18)
4: Form Ξ using k samples with the smallest cosine distance to $\hat{\mathbf{z}}_*$ in $\hat{\mathbf{Z}}$
5: Obtain output labels according to Eq.(20)
Output: Predicted labels for the testing sample \mathbf{x}_*

where $\Delta = \mathbf{W}^{(t+1)} - \mathbf{W}^{(t)}$ is the update step, $\nabla \mathcal{L}'(\mathbf{W}^{(t)})$ and $\mathcal{H}(\mathbf{W}^{(t)})$ are the gradient and Hessian matrix of $\mathcal{L}'(\mathbf{W}^{(t)})$ at $\mathbf{W}^{(t)}$, respectively. Then the minimizer of Eq.(11) is

$$\Delta^{(t)} = -\mathcal{H}^{-1}(\mathbf{W}^{(t)}) \nabla \mathcal{L}'(\mathbf{W}^{(t)}). \quad (12)$$

The line search Newton method utilizes $\Delta^{(t)}$ as the search direction, denoted as $\mathbf{D}^{(t)} = \Delta^{(t)}$, and the model parameters are updated using:

$$\mathbf{W}^{(t+1)} = \mathbf{W}^{(t)} + \beta^{(t)} \mathbf{D}^{(t)}, \quad (13)$$

where the step length $\beta^{(t)}$ is determined through a line search procedure to satisfy the strong Wolfe conditions [79]:

$$\mathcal{L}'(\mathbf{W}^{(t)} + \beta^{(t)} \mathbf{D}^{(t)}) \leq \mathcal{L}'(\mathbf{W}^{(t)}) + c_1 \beta^{(t)} \nabla \mathcal{L}'(\mathbf{W}^{(t)})^T \mathbf{D}^{(t)}, \quad (14)$$

$$\left| \nabla \mathcal{L}'(\mathbf{W}^{(t)} + \beta^{(t)} \mathbf{D}^{(t)}) \right| \leq c_2 \left| \nabla \mathcal{L}'(\mathbf{W}^{(t)})^T \mathbf{D}^{(t)} \right|, \quad (15)$$

where $0 < c_1 < c_2 < 1$. The L-BFGS algorithm aims to avoid the explicit calculation of $\mathcal{H}^{-1}(\mathbf{W}^{(t)})$ by approximating it with an iteratively updated matrix \mathbf{B} , i.e.,

$$\begin{aligned} & \mathbf{B}^{(t+1)} \\ &= \left(\mathbf{I} - \Lambda^{(t)} \mathbf{S}^{(t)} (\mathbf{U}^{(t)})^T \right) \mathbf{B}^{(t)} \left(\mathbf{I} - \Lambda^{(t)} \mathbf{S}^{(t)} (\mathbf{U}^{(t)})^T \right) \\ & \quad + \Lambda^{(t)} \mathbf{S}^{(t)} (\mathbf{U}^{(t)})^T, \end{aligned} \quad (16)$$

where \mathbf{I} is the identity matrix, $\mathbf{S} = \mathbf{W}^{(t+1)} - \mathbf{W}^{(t)}$, $\mathbf{U}^{(t)} = \nabla \mathcal{L}'(\mathbf{W}^{(t+1)}) - \nabla \mathcal{L}'(\mathbf{W}^{(t)})$, and $\Lambda^{(t)} = \frac{1}{\mathbf{S}^{(t)} \mathbf{U}^{(t)}}$.

We use m to denote the learning iterations of L-BFGS and N to denote the number of samples, then the computational complexity of the training process of SLDL is $\mathcal{O}(mNq\hat{c})$, which is no longer associated with the number of labels.

2) *Model Prediction:* In the prediction process, SLDL first calculate the embedding matrix $\hat{\mathbf{Z}}$ of training samples transformed by \mathbf{W} :

$$\hat{\mathbf{Z}} = \mathbf{X} \mathbf{W}. \quad (17)$$

For a new sample \mathbf{x}_* , SLDL first calculates its corresponding target vector in the embedding space $\hat{\mathbf{z}}_*$:

$$\hat{\mathbf{z}}_* = \mathbf{x}_* \mathbf{W}. \quad (18)$$

After that, a decoder is employed to map the target embedding vector to the predicted label vector. For simplicity, SLDL adopts a Nearest Neighbor-based decoding method. The cosine distance of the new sample $\hat{\mathbf{z}}_*$ to the i -th sample $\hat{\mathbf{z}}_i$ in $\hat{\mathbf{Z}}$ is calculated by

$$d_i = 1 - \frac{\hat{\mathbf{z}}_* \cdot \hat{\mathbf{z}}_i}{\|\hat{\mathbf{z}}_*\| \|\hat{\mathbf{z}}_i\|}. \quad (19)$$

Subsequently, by utilizing the reciprocal of the cosine distance as the weight, SLDL acquires the weighted sum of the original label vectors corresponding to the samples with the smallest cosine distance to $\hat{\mathbf{z}}_*$ in $\hat{\mathbf{Z}}$:

$$\hat{\mathbf{y}}_* = \sum_{i \in \Xi} \frac{\mathbf{y}_i}{d_i}, \quad (20)$$

where Ξ represents the index set corresponding to k samples with the smallest cosine distance to $\hat{\mathbf{z}}_*$ in $\hat{\mathbf{Z}}$. Finally, SLDL selects the labels with top- k scores for model prediction. The pseudocode of the training algorithm and test algorithm is given in algorithm 2 and algorithm 3, respectively.

E. Theoretical Analysis

We study the theoretical guarantees of SLDL to reveal the effectiveness of Gaussian embedding with asymmetric metrics below. Let \mathcal{C} be the possible cost function for measure the penalty between the ground-truth label vector \mathbf{y} and the predicted label vector $\hat{\mathbf{y}}$. We assume $\mathcal{C}(\mathbf{y}, \hat{\mathbf{y}}) \geq 0$ iff \mathbf{y} and $\hat{\mathbf{y}}$ are the same. Then we have the following theorem:

Theorem 1. *For any sample (\mathbf{x}, \mathbf{y}) , let \mathbf{z} be the embedding vector of \mathbf{y} , $\hat{\mathbf{z}}$ be the predicted embedding vector, and $\tilde{\mathbf{z}}$ be the nearest embedding vector of $\hat{\mathbf{z}}$. Then the following bound holds*

$$\mathcal{C}(\mathbf{y}, \hat{\mathbf{y}}) \leq b \left(\mathcal{D}(\mathbf{z}, \tilde{\mathbf{z}}) - \mathcal{C}(\mathbf{y}, \hat{\mathbf{y}})^{\frac{1}{2}} \right)^2 + b \mathcal{D}(\mathbf{z}, \hat{\mathbf{z}})^2, \quad (21)$$

where $\mathcal{D}(\cdot, \cdot)$ denotes Euclidean distance and $b > 1$ is a constant.

TABLE I: Statistics of multi-label classification benchmark datasets.

No.	Dataset	Number of samples	Number of feature dimensions	Number of labels
1	cal500	502	68	174
2	corel16k-s1	13766	500	153
3	corel16k-s2	13761	500	164
4	corel16k-s3	13760	500	154
5	CUB	11788	128	312
6	delicious	16105	500	983
7	eurlex-dc	19348	500	412
8	eurlex-sm	19348	500	201
9	espgame	20770	1000	268
10	stackex-chemistry	6961	540	175
11	stackex-chess	1675	585	227
12	stackex-coffee	225	1763	123
13	stackex-cooking	10491	577	400
14	stackex-cs	9270	635	274
15	stackex-philosophy	3971	842	233

TABLE II: Experimental results (mean \pm std) on the MLC benchmark datasets measured by P@1 (nDCG@1). ●/○ indicates whether SLDL is statistically superior/inferior to the comparing methods.

Dataset	SLEEC [38]	DXML [52]	Focal [45]	CB [47]	DB [43]	PACA [31]	FLEM [22]	DELA [21]	CLIF [19]	SLDL (Ours)
cal500	86.66±3.16●	86.45±2.51●	87.85±3.11●	87.85±3.82●	85.45±4.10●	88.05±3.42●	88.45±2.46	85.07±4.64●	84.67±4.58●	88.45±2.11
corel16k-s1	36.53±1.37●	31.70±0.94●	32.64±0.85●	32.58±1.01●	30.01±0.76●	28.38±1.71●	35.97±1.13●	27.89±0.70●	27.03±1.19●	37.86±0.85
corel16k-s2	36.60±1.05●	31.54±0.96●	33.26±0.66●	33.12±0.77●	30.22±1.26●	28.76±1.56●	36.58±1.04●	28.30±0.79●	27.05±1.04●	37.79±1.00
corel16k-s3	36.29±1.41●	31.96±1.26●	32.49±1.65●	32.64±1.62●	29.65±1.84●	28.53±1.71●	35.52±1.35●	27.88±1.28●	26.87±1.33●	37.80±1.51
CUB	86.02±1.53●	84.39±0.95●	86.28±1.06●	86.49±1.06●	86.11±1.38●	86.18±0.94●	84.96±0.64●	87.05±1.16●	83.90±1.19●	87.13±1.06
delicious	67.49±0.87●	59.83±1.12●	65.68±0.92●	65.61±0.90●	62.59±0.73●	65.84±1.01●	67.15±0.48●	65.05±0.94●	61.34±0.77●	67.67±0.96
eurlex-dc	54.41±1.36●	54.33±0.85●	26.40±1.37●	26.30±1.41●	27.26±1.49●	45.33±2.79●	22.46±1.43●	45.83±1.39●	58.89±1.19●	62.03±1.34
eurlex-sm	64.34±1.46●	68.54±1.18●	35.50±1.54●	35.52±1.55●	29.83±1.14●	67.21±1.78●	31.49±1.39●	62.70±1.33●	75.39±0.96	74.77±1.49
espgame	37.69±1.13●	31.35±1.42●	35.21±1.61●	35.45±1.53●	33.29±1.40●	37.47±1.62●	37.78±1.52●	33.83±1.28●	32.01±0.85●	41.89±1.36
stackex-chemistry	23.23±1.37●	28.89±1.18●	38.56±1.73●	38.40±1.87●	36.99±1.44●	35.57±1.57●	35.10±2.08●	38.73±1.83●	36.29±1.72●	44.74±1.18
stackex-chess	29.38±3.98●	52.77±4.15●	44.06±3.39●	45.07±4.41●	41.49±2.62●	41.55±2.88●	39.82±3.48●	46.68±4.53●	44.24±3.96●	55.40±4.77
stackex-coffee	41.40±12.06●	29.72±9.35●	22.31±10.80●	24.01±10.44●	25.45±14.38●	17.81±7.58●	24.90±14.01●	28.06±9.42●	29.88±11.79●	45.32±10.70
stackex-cooking	22.93±0.98●	30.68±6.91●	44.10±1.69●	44.26±1.61●	42.61±1.73●	44.00±1.51●	37.82±1.25●	49.27±1.64●	45.76±1.02●	57.46±0.88
stackex-cs	29.44±1.22●	43.79±1.49●	50.76±2.08●	50.70±2.12●	51.45±1.81●	48.28±2.02●	46.80±1.92●	51.31±2.08●	48.30±1.62●	55.95±2.36
stackex-philosophy	22.59±2.21●	48.50±2.67●	41.15±2.50●	41.05±2.14●	38.30±2.57●	39.03±3.26●	37.98±2.23●	44.67±2.20●	43.54±1.91●	53.64±2.78
Avg. Rank	5.60	6.40	5.33	5.27	6.93	6.27	6.07	5.40	6.53	1.07

Proof. Since \tilde{z} is the nearest neighbor of \hat{z} , we define $\mathcal{D}(z, \tilde{z}) \leq (b-1)\mathcal{D}(z, \hat{z})$ that bounds the distance of z and \tilde{z} [80]. Then we have:

$$\begin{aligned}
& \left(\mathcal{D}(z, \tilde{z}) - (\mathcal{C}(\mathbf{y}, \hat{\mathbf{y}}))^{\frac{1}{2}} \right)^2 + \mathcal{D}(z, \hat{z})^2 \\
& \geq \left(\mathcal{D}(z, \tilde{z}) - (\mathcal{C}(\mathbf{y}, \hat{\mathbf{y}}))^{\frac{1}{2}} \right)^2 + \frac{1}{b-1} \mathcal{D}(z, \tilde{z})^2 \\
& = \frac{b}{b-1} \left(\mathcal{D}(z, \tilde{z}) - \frac{b-1}{b} (\mathcal{C}(\mathbf{y}, \hat{\mathbf{y}}))^{\frac{1}{2}} \right)^2 + \frac{1}{b} \mathcal{C}(\mathbf{y}, \hat{\mathbf{y}}) \\
& \geq \frac{1}{b} \mathcal{C}(\mathbf{y}, \hat{\mathbf{y}}),
\end{aligned} \tag{22}$$

which finishes the proof. \square

Theorem 1 demonstrates that the cost function of SLDL can be bounded by the sum of embedding error $\left(\mathcal{D}(z, \tilde{z}) - \mathcal{C}(\mathbf{y}, \hat{\mathbf{y}})^{\frac{1}{2}} \right)^2$ and regression error $\mathcal{D}(z, \hat{z})^2$, which indicates that superior embedding learning approach can effectively improve the performance of the model. As we can observe in Section IV-E1 below, our embedding method has significant advantages over vanilla embedding approaches that use the mean square error loss function, which proves the effectiveness of our proposed method.

IV. EXPERIMENTS

In this section, we evaluate the efficiency and performance of SLDL across multiple multi-label classification datasets. All methods are implemented using PyTorch, and the experiments are performed on a GPU server equipped with an NVIDIA Tesla V100 GPU, AMD Ryzen 7 5800X processor CPU, and 32 GB GPU memory. To evaluate the proposed approach, we conduct experiments on fifteen benchmark datasets widely employed in multi-label classification research. The details of these datasets provided in Table I.

A. Comparing Algorithms

We compare our proposed methods with several state-of-the-art MLC technologies. The compared methods include:

- *Sparse local embeddings for extreme classification* (SLEEC) [38]: a multi-label classification method specifically proposed for MLC tasks with large-scale output space. SLEEC aims to embed labels by preserving the pairwise distances between a few nearest label neighbors. In the experiments, the embedding dimension is set to 100, the number of neighbors for embedding is set to

TABLE III: Experimental results (mean \pm std) on the MLC benchmark datasets measured by P@3. \bullet/\circ indicates whether SLDL is statistically superior/inferior to the comparing methods.

Dataset	SLEEC [38]	DXML [52]	Focal [45]	CB [47]	DB [43]	PACA [31]	FLEM [22]	DELA [21]	CLIF [19]	SLDL (Ours)
cal500	73.04 \pm 2.92 \bullet	73.50 \pm 2.76 \bullet	74.16 \pm 4.03 \bullet	74.95 \pm 4.92 \bullet	72.43 \pm 3.41 \bullet	74.89 \pm 3.55 \bullet	74.83 \pm 3.33 \bullet	72.97 \pm 4.15 \bullet	72.90 \pm 4.31 \bullet	76.10\pm2.59
corel16k-s1	27.37 \pm 0.91 \bullet	24.23 \pm 0.71 \bullet	25.23 \pm 0.45 \bullet	25.29 \pm 0.36 \bullet	22.95 \pm 0.43 \bullet	20.87 \pm 0.99 \bullet	27.32 \pm 0.43 \bullet	20.87 \pm 0.51 \bullet	20.46 \pm 0.64 \bullet	28.39\pm0.67
corel16k-s2	27.46 \pm 0.79 \bullet	24.26 \pm 0.58 \bullet	25.53 \pm 0.82 \bullet	25.51 \pm 0.71 \bullet	23.09 \pm 0.62 \bullet	21.51 \pm 0.85 \bullet	27.63 \pm 0.69 \bullet	21.27 \pm 0.45 \bullet	20.58 \pm 0.73 \bullet	28.59\pm0.77
corel16k-s3	27.32 \pm 1.05 \bullet	24.39 \pm 0.96 \bullet	25.22 \pm 0.99 \bullet	25.33 \pm 1.06 \bullet	22.84 \pm 0.95 \bullet	20.91 \pm 1.24 \bullet	27.50 \pm 0.99 \bullet	20.83 \pm 0.85 \bullet	20.25 \pm 0.85 \bullet	28.36\pm0.86
CUB	80.20 \pm 1.02 \bullet	74.48 \pm 0.97 \bullet	79.14 \pm 0.90 \bullet	79.42 \pm 0.96 \bullet	79.80 \pm 0.95 \bullet	79.95 \pm 0.99 \bullet	77.73 \pm 0.80 \bullet	81.28\pm0.77\circ	78.32 \pm 1.08 \bullet	80.27 \pm 0.86
delicious	61.43 \pm 0.85 \bullet	53.45 \pm 0.98 \bullet	59.91 \pm 0.40 \bullet	59.86 \pm 0.51 \bullet	57.23 \pm 0.67 \bullet	59.92 \pm 0.91 \bullet	61.33 \pm 0.44 \bullet	59.66 \pm 0.68 \bullet	55.78 \pm 1.01 \bullet	62.13\pm0.72
eurlex-dc	26.64 \pm 0.52 \bullet	26.56 \pm 0.38 \bullet	12.28 \pm 0.51 \bullet	12.26 \pm 0.52 \bullet	13.21 \pm 0.48 \bullet	21.32 \pm 1.05 \bullet	11.14 \pm 0.48 \bullet	22.35 \pm 0.59 \bullet	27.59 \pm 0.53 \bullet	28.68\pm0.45
eurlex-sm	44.82 \pm 1.04 \bullet	46.48 \pm 0.81 \bullet	28.47 \pm 0.93 \bullet	28.45 \pm 0.90 \bullet	25.38 \pm 1.12 \bullet	44.34 \pm 1.11 \bullet	25.89 \pm 0.71 \bullet	41.63 \pm 0.99 \bullet	50.01 \pm 0.70 \bullet	50.63\pm0.92
espgame	29.73 \pm 0.48 \bullet	24.47 \pm 0.69 \bullet	28.53 \pm 0.81 \bullet	28.65 \pm 0.76 \bullet	26.41 \pm 0.83 \bullet	28.62 \pm 1.13 \bullet	30.34 \pm 0.69 \bullet	27.03 \pm 0.55 \bullet	25.81 \pm 0.62 \bullet	33.76\pm0.31
stackex-chemistry	16.29 \pm 0.44 \bullet	19.49 \pm 0.78 \bullet	26.29 \pm 0.82 \bullet	26.33 \pm 0.70 \bullet	24.92 \pm 0.88 \bullet	23.16 \pm 0.76 \bullet	23.67 \pm 0.74 \bullet	25.80 \pm 0.69 \bullet	23.68 \pm 0.99 \bullet	28.27\pm0.68
stackex-chess	19.58 \pm 1.28 \bullet	31.78 \pm 2.41 \bullet	27.62 \pm 1.74 \bullet	27.74 \pm 1.68 \bullet	27.20 \pm 1.55 \bullet	25.89 \pm 1.69 \bullet	25.51 \pm 1.50 \bullet	29.00 \pm 1.80 \bullet	28.58 \pm 1.89 \bullet	32.93\pm2.53
stackex-coffee	30.99\pm5.54	19.98 \pm 3.71 \bullet	16.79 \pm 4.99 \bullet	16.05 \pm 4.40 \bullet	17.54 \pm 4.73 \bullet	13.37 \pm 3.93 \bullet	17.36 \pm 6.61 \bullet	22.42 \pm 7.16 \bullet	20.95 \pm 5.99 \bullet	30.08 \pm 5.30
stackex-cooking	14.71 \pm 0.49 \bullet	19.48 \pm 3.45 \bullet	27.98 \pm 0.79 \bullet	27.99 \pm 0.72 \bullet	26.82 \pm 0.78 \bullet	25.73 \pm 0.87 \bullet	24.42 \pm 0.53 \bullet	29.11 \pm 0.62 \bullet	27.28 \pm 0.52 \bullet	31.99\pm0.41
stackex-cs	19.99 \pm 0.64 \bullet	30.44 \pm 0.68 \bullet	36.67 \pm 0.71 \bullet	36.76 \pm 0.67 \bullet	36.22 \pm 0.75 \bullet	33.34 \pm 0.96 \bullet	33.74 \pm 0.56 \bullet	36.53 \pm 0.87 \bullet	34.57 \pm 1.01 \bullet	39.14\pm0.75
stackex-philosophy	15.69 \pm 0.86 \bullet	28.83 \pm 0.56 \bullet	25.95 \pm 0.61 \bullet	25.88 \pm 0.82 \bullet	25.15 \pm 0.94 \bullet	23.80 \pm 0.86 \bullet	23.13 \pm 0.83 \bullet	26.76 \pm 0.89 \bullet	26.88 \pm 1.02 \bullet	31.25\pm0.72
Avg. Rank	5.40	6.47	5.40	5.00	7.00	6.67	6.07	5.33	6.47	1.13

TABLE IV: Experimental results (mean \pm std) on the MLC benchmark datasets measured by P@5. \bullet/\circ indicates whether SLDL is statistically superior/inferior to the comparing methods.

Dataset	SLEEC [38]	DXML [52]	Focal [45]	CB [47]	DB [43]	PACA [31]	FLEM [22]	DELA [21]	CLIF [19]	SLDL (Ours)
cal500	68.44 \pm 3.15 \bullet	67.80 \pm 3.51 \bullet	68.00 \pm 3.53 \bullet	68.17 \pm 3.30 \bullet	65.97 \pm 2.54 \bullet	67.87 \pm 3.16 \bullet	68.56 \pm 2.65 \bullet	67.17 \pm 3.15 \bullet	67.33 \pm 4.33 \bullet	69.64\pm3.21
corel16k-s1	22.24 \pm 0.61 \bullet	19.99 \pm 0.69 \bullet	20.82 \pm 0.33 \bullet	20.82 \pm 0.31 \bullet	19.15 \pm 0.41 \bullet	17.04 \pm 0.75 \bullet	22.45 \pm 0.42 \bullet	17.11 \pm 0.32 \bullet	16.69 \pm 0.53 \bullet	23.40\pm0.42
corel16k-s2	22.31 \pm 0.62 \bullet	19.94 \pm 0.47 \bullet	21.03 \pm 0.55 \bullet	21.02 \pm 0.58 \bullet	19.22 \pm 0.36 \bullet	17.69 \pm 0.54 \bullet	22.67 \pm 0.58 \bullet	17.33 \pm 0.42 \bullet	16.93 \pm 0.65 \bullet	23.46\pm0.65
corel16k-s3	22.31 \pm 0.60 \bullet	20.01 \pm 0.64 \bullet	21.03 \pm 0.63 \bullet	21.02 \pm 0.60 \bullet	19.19 \pm 0.67 \bullet	17.15 \pm 0.95 \bullet	22.56 \pm 0.71 \bullet	17.09 \pm 0.56 \bullet	16.67 \pm 0.56 \bullet	23.37\pm0.58
CUB	76.56 \pm 0.94 \bullet	69.25 \pm 1.10 \bullet	75.26 \pm 1.03 \bullet	75.39 \pm 1.18 \bullet	75.93 \pm 0.96 \bullet	75.97 \pm 0.98 \bullet	73.35 \pm 0.71 \bullet	77.59\pm0.72\circ	74.90 \pm 1.15 \bullet	76.45 \pm 0.83
delicious	56.59 \pm 0.82 \bullet	48.73 \pm 0.95 \bullet	55.36 \pm 0.47 \bullet	55.28 \pm 0.57 \bullet	52.78 \pm 0.55 \bullet	55.34 \pm 0.77 \bullet	56.62 \pm 0.50 \bullet	55.06 \pm 0.64 \bullet	51.51 \pm 0.78 \bullet	57.64\pm0.68
eurlex-dc	17.71 \pm 0.35 \bullet	18.05 \pm 0.25 \bullet	8.71 \pm 0.33 \bullet	8.69 \pm 0.34 \bullet	9.08 \pm 0.28 \bullet	14.65 \pm 0.61 \bullet	7.89 \pm 0.30 \bullet	15.44 \pm 0.22 \bullet	18.43 \pm 0.30 \bullet	18.68\pm0.30
eurlex-sm	31.52 \pm 0.64 \bullet	32.83 \pm 0.59 \bullet	19.49 \pm 0.66 \bullet	19.48 \pm 0.67 \bullet	19.88 \pm 0.68 \bullet	30.73 \pm 0.66 \bullet	17.66 \pm 0.57 \bullet	29.25 \pm 0.65 \bullet	34.35\pm0.41	34.31 \pm 0.55
espgame	25.08 \pm 0.36 \bullet	20.83 \pm 0.40 \bullet	24.56 \pm 0.43 \bullet	24.58 \pm 0.46 \bullet	22.69 \pm 0.52 \bullet	24.00 \pm 0.61 \bullet	25.89 \pm 0.42 \bullet	22.75 \pm 0.44 \bullet	21.76 \pm 0.39 \bullet	28.37\pm0.40
stackex-chemistry	13.08 \pm 0.28 \bullet	15.25 \pm 0.63 \bullet	20.25 \pm 0.57 \bullet	20.19 \pm 0.63 \bullet	19.34 \pm 0.43 \bullet	17.69 \pm 0.56 \bullet	18.22 \pm 0.43 \bullet	19.54 \pm 0.60 \bullet	18.19 \pm 0.55 \bullet	21.20\pm0.37
stackex-chess	15.58 \pm 1.02 \bullet	23.63 \pm 1.60 \bullet	20.94 \pm 0.98 \bullet	21.21 \pm 1.08 \bullet	20.64 \pm 1.21 \bullet	19.80 \pm 1.35 \bullet	19.84 \pm 1.03 \bullet	21.73 \pm 1.01 \bullet	21.42 \pm 1.18 \bullet	24.24\pm1.38
stackex-coffee	22.40 \pm 2.38 \bullet	15.72 \pm 2.86 \bullet	12.55 \pm 3.23 \bullet	11.95 \pm 3.34 \bullet	13.29 \pm 3.37 \bullet	10.96 \pm 2.80 \bullet	13.26 \pm 4.06 \bullet	17.45 \pm 3.58 \bullet	15.68 \pm 3.58 \bullet	22.67\pm2.97
stackex-cooking	11.30 \pm 0.29 \bullet	14.64 \pm 2.15 \bullet	20.48 \pm 0.35 \bullet	20.47 \pm 0.37 \bullet	19.75 \pm 0.38 \bullet	18.75 \pm 0.66 \bullet	18.30 \pm 0.34 \bullet	20.96 \pm 0.30 \bullet	19.66 \pm 0.45 \bullet	22.59\pm0.23
stackex-cs	15.79 \pm 0.51 \bullet	22.99 \pm 0.62 \bullet	27.87 \pm 0.52 \bullet	27.78 \pm 0.49 \bullet	27.29 \pm 0.38 \bullet	25.29 \pm 0.59 \bullet	25.54 \pm 0.29 \bullet	27.80 \pm 0.59 \bullet	26.25 \pm 0.70 \bullet	28.95\pm0.47
stackex-philosophy	12.94 \pm 0.60 \bullet	21.12 \pm 0.52 \bullet	19.54 \pm 0.50 \bullet	19.53 \pm 0.43 \bullet	19.43 \pm 0.49 \bullet	17.56 \pm 0.84 \bullet	17.56 \pm 0.47 \bullet	19.45 \pm 0.39 \bullet	19.66 \pm 0.54 \bullet	22.69\pm0.56
Avg. Rank	5.33	6.40	4.93	5.47	6.73	7.13	5.67	5.47	6.53	1.20

250, and the number of neighbors for prediction is set to 25 as suggested in the code provided by the authors.

- *Deep extreme multi-label learning* (DXML) [52]: a deep embedding method specifically proposed for multi-label classification tasks with large-scale output space. It integrates the concepts of non-linear embedding and graph priors-based label space modeling simultaneously. In the experiments, the embedding dimension is set to 300 as suggested by the original paper.
- *Focal loss* (FL) [45]: a simple yet commonly used approach in classification tasks. It elevates the loss weight for instances that are hard to classify, particularly those predicted with low probability on the ground-truth. We apply a balance parameter of 2 and set $\gamma = 2$ for focal loss, following the suggestion in [43].
- *Class-balanced loss* (CB) [47]: a balancing method that adjusts weights for each class based on their effective number, represented as $E_n = (1 - \beta^n)/(1 - \beta)$. It further reweights focal loss, capturing diminishing marginal benefits of data and consequently reducing redundant

information from head classes.

- *Distribution balance loss* (DB) [43]: a specialized balancing loss crafted for multi-label classification tasks. It strategically mitigates label co-occurrence redundancy, crucial in the multi-label scenario, and selectively assigns lower weights to “easy-to-classify” negative instances through a combination of rebalanced weighting and negative-tolerant regularization.
- *Probabilistic label-specific feature learning* (PACA) [31]: a multi-label classification method that transforms features based on label-specific prototypes in an end-to-end manner. In the experiments, α and γ are set to 1 as suggested in the code provided by the authors.
- *Fusion label enhancement for multi-label learning* (FLEM) [22]: a label-enhancement-based multi-label classification method that integrates the label enhancement process and the multi-label classification training process. In the experiments, α and β are set to 0.01 as suggested in the official code.
- *Dual perspective of label-specific feature learning*

TABLE V: Experimental results (mean \pm std) on the MLC benchmark datasets measured by nDCG@3. \bullet/\circ indicates whether SLDL is statistically superior/inferior to the comparing methods.

Dataset	SLEEC [38]	DXML [52]	Focal [45]	CB [47]	DB [43]	PACA [31]	FLEM [22]	DELA [21]	CLIF [19]	SLDL (Ours)
cal500	75.98 \pm 2.48	76.23 \pm 2.48	77.18 \pm 3.32	77.78 \pm 4.15	75.17 \pm 3.22	77.51 \pm 3.19	77.79 \pm 2.89	75.51 \pm 4.04	75.44 \pm 4.00	78.30\pm2.62
corel16k-s1	32.64 \pm 1.01	28.75 \pm 0.75	29.78 \pm 0.44	29.81 \pm 0.36	27.42 \pm 0.51	25.02 \pm 1.24	32.44 \pm 0.56	24.72 \pm 0.60	24.28 \pm 0.80	33.68\pm0.76
corel16k-s2	32.40 \pm 0.90	28.34 \pm 0.50	29.81 \pm 0.79	29.78 \pm 0.71	27.36 \pm 0.81	25.34 \pm 0.97	32.43 \pm 0.76	24.90 \pm 0.53	24.09 \pm 0.85	33.39\pm0.89
corel16k-s3	32.52 \pm 1.16	28.79 \pm 1.14	29.76 \pm 1.11	29.87 \pm 1.10	27.42 \pm 1.19	25.02 \pm 1.44	32.51 \pm 1.07	24.77 \pm 0.86	24.06 \pm 0.96	33.60\pm1.14
CUB	81.52 \pm 1.06	76.65 \pm 0.86	80.77 \pm 0.84	81.03 \pm 0.94	81.24 \pm 1.00	81.37 \pm 0.93	79.39 \pm 0.74	82.59\pm0.81	79.60 \pm 1.06	81.80 \pm 0.89
delicious	62.88 \pm 0.85	54.96 \pm 1.00	61.28 \pm 0.48	61.23 \pm 0.56	58.52 \pm 0.63	61.36 \pm 0.88	62.74 \pm 0.42	60.97 \pm 0.68	57.10 \pm 0.94	63.39\pm0.74
eurlex-dc	60.80 \pm 1.17	60.81 \pm 0.87	29.90 \pm 1.27	29.84 \pm 1.29	31.87 \pm 1.28	49.90 \pm 2.63	26.74 \pm 1.22	51.54 \pm 1.28	63.87 \pm 1.02	66.64\pm1.04
eurlex-sm	62.85 \pm 1.23	66.09 \pm 0.86	35.89 \pm 1.07	35.87 \pm 1.06	34.08 \pm 1.19	63.36 \pm 1.64	32.61 \pm 0.91	58.72 \pm 1.10	72.05 \pm 0.69	72.30\pm1.04
espgame	32.55 \pm 0.58	26.81 \pm 0.86	30.95 \pm 1.08	31.10 \pm 1.01	28.94 \pm 1.00	31.61 \pm 1.33	33.00 \pm 0.96	29.56 \pm 0.75	28.15 \pm 0.72	36.90\pm0.50
stackex-chemistry	23.92 \pm 0.62	28.70 \pm 0.93	38.97 \pm 0.97	38.93 \pm 0.96	37.19 \pm 1.11	34.74 \pm 1.07	35.16 \pm 1.23	38.60 \pm 0.90	35.52 \pm 1.35	42.82\pm0.60
stackex-chess	26.80 \pm 2.42	45.57 \pm 3.47	38.97 \pm 2.87	38.92 \pm 3.19	38.07 \pm 2.39	36.34 \pm 2.18	35.73 \pm 2.67	41.12 \pm 2.89	39.91 \pm 2.94	47.07\pm4.16
stackex-coffee	49.07\pm10.20	32.39 \pm 7.94	26.30 \pm 9.30	26.41 \pm 7.53	27.79 \pm 8.13	20.21 \pm 6.55	27.92 \pm 10.56	34.94 \pm 10.84	33.31 \pm 9.31	48.35 \pm 9.28
stackex-cooking	21.15 \pm 0.56	28.13 \pm 5.47	40.30 \pm 0.97	40.32 \pm 1.00	38.82 \pm 1.18	38.22 \pm 1.33	34.92 \pm 0.66	43.08 \pm 1.00	40.18 \pm 0.98	48.16\pm0.75
stackex-cs	25.64 \pm 1.01	39.02 \pm 0.92	46.98 \pm 1.13	47.00 \pm 0.95	46.96 \pm 1.08	43.26 \pm 1.35	42.93 \pm 1.04	47.37 \pm 1.31	44.65 \pm 1.37	50.63\pm1.76
stackex-philosophy	23.40 \pm 1.61	44.57 \pm 1.48	39.15 \pm 1.53	39.09 \pm 1.66	37.73 \pm 1.69	36.06 \pm 1.90	35.53 \pm 1.66	40.76 \pm 1.86	40.37 \pm 1.55	48.16\pm0.93
Avg. Rank	5.47	6.40	5.47	5.20	7.00	6.53	6.07	5.20	6.53	1.13

TABLE VI: Experimental results (mean \pm std) on the MLC benchmark datasets measured by nDCG@5. \bullet/\circ indicates whether SLDL is statistically superior/inferior to the comparing methods.

Dataset	SLEEC [38]	DXML [52]	Focal [45]	CB [47]	DB [43]	PACA [31]	FLEM [22]	DELA [21]	CLIF [19]	SLDL (Ours)
cal500	72.00 \pm 2.61	71.56 \pm 2.98	72.08 \pm 3.15	72.33 \pm 3.32	69.98 \pm 2.61	71.97 \pm 2.80	72.63 \pm 2.44	70.77 \pm 3.17	70.90 \pm 3.98	73.33\pm2.65
corel16k-s1	36.63 \pm 0.93	32.56 \pm 0.97	33.78 \pm 0.47	33.78 \pm 0.42	31.34 \pm 0.56	28.16 \pm 1.30	36.70 \pm 0.62	27.91 \pm 0.57	27.34 \pm 0.91	38.16\pm0.56
corel16k-s2	36.07 \pm 1.01	31.83 \pm 0.57	33.52 \pm 0.77	33.47 \pm 0.77	30.96 \pm 0.67	28.43 \pm 0.94	36.34 \pm 0.87	27.80 \pm 0.60	27.04 \pm 0.99	37.42\pm1.05
corel16k-s3	36.43 \pm 1.11	32.41 \pm 1.13	33.79 \pm 1.09	33.83 \pm 1.01	31.30 \pm 1.25	28.10 \pm 1.50	36.53 \pm 1.13	27.82 \pm 0.86	27.06 \pm 0.89	37.80\pm1.15
CUB	78.68 \pm 0.99	72.46 \pm 0.94	77.66 \pm 0.95	77.81 \pm 1.09	78.20 \pm 1.00	78.25 \pm 0.92	75.93 \pm 0.70	79.71\pm0.75	76.90 \pm 1.05	78.77 \pm 0.86
delicious	59.30 \pm 0.82	51.39 \pm 0.96	57.91 \pm 0.49	57.84 \pm 0.56	55.27 \pm 0.56	57.96 \pm 0.77	59.26 \pm 0.45	57.57 \pm 0.58	53.94 \pm 0.79	60.09\pm0.70
eurlex-dc	63.46 \pm 1.24	64.07 \pm 0.84	32.30 \pm 1.28	32.23 \pm 1.33	33.90 \pm 1.24	52.88 \pm 2.60	29.00 \pm 1.19	54.74 \pm 1.03	66.75 \pm 0.95	68.81\pm1.04
eurlex-sm	66.76 \pm 1.15	70.25 \pm 0.82	37.52 \pm 1.18	37.52 \pm 1.19	38.56 \pm 1.19	66.69 \pm 1.52	34.04 \pm 1.01	62.34 \pm 1.12	75.35\pm0.53	75.18 \pm 0.97
espgame	31.46 \pm 0.52	26.00 \pm 0.67	30.38 \pm 0.86	30.44 \pm 0.85	28.41 \pm 0.90	30.53 \pm 1.02	32.16 \pm 0.77	28.63 \pm 0.73	27.34 \pm 0.57	35.78\pm0.53
stackex-chemistry	27.40 \pm 0.66	32.35 \pm 0.96	43.44 \pm 1.02	43.34 \pm 1.07	41.60 \pm 0.98	38.47 \pm 1.25	39.30 \pm 1.11	42.61 \pm 1.01	39.51 \pm 1.20	46.72\pm0.83
stackex-chess	29.60 \pm 2.49	48.36 \pm 2.99	41.75 \pm 2.35	42.43 \pm 2.96	40.94 \pm 2.57	38.93 \pm 1.87	39.04 \pm 2.37	43.84 \pm 2.39	42.54 \pm 2.61	49.40\pm3.55
stackex-coffee	54.26\pm8.60	37.42 \pm 8.56	29.87 \pm 8.98	29.71 \pm 8.43	31.35 \pm 8.62	24.59 \pm 6.80	31.70 \pm 10.61	40.23 \pm 9.80	37.21 \pm 9.37	53.10 \pm 8.71
stackex-cooking	23.47 \pm 0.51	30.78 \pm 5.46	43.45 \pm 0.84	43.47 \pm 0.92	42.02 \pm 1.12	41.03 \pm 1.44	38.22 \pm 0.73	45.94 \pm 0.86	42.92 \pm 1.17	50.58\pm0.77
stackex-cs	28.34 \pm 1.09	42.14 \pm 0.98	50.91 \pm 1.09	50.79 \pm 0.99	50.55 \pm 0.83	46.72 \pm 1.14	46.38 \pm 0.95	51.30 \pm 1.20	48.30 \pm 1.40	53.88\pm1.65
stackex-philosophy	26.83 \pm 1.52	47.30 \pm 1.28	42.36 \pm 1.45	42.28 \pm 1.37	41.32 \pm 1.39	38.51 \pm 2.07	38.47 \pm 1.38	43.18 \pm 1.55	42.95 \pm 1.26	50.87\pm1.14
Avg. Rank	5.40	6.40	5.27	5.33	6.87	6.80	5.87	5.27	6.47	1.20

(DELA) [21]: a label-specific feature learning approach with a dual perspective for multi-label classification. In the experiments, β is set to 1 as suggested in the code provided by the authors.

- *Collaborative learning of label semantics and deep label-specific features* (CLIF) [19]: a multi-label classification method that learns label semantics and label-specific features in a collaborative way. In the experiments, the maximum number of iterations is set to 100, λ is set to 0.01 as suggested in the code provided by the authors.

B. Evaluation Metrics

We evaluate the performance of the algorithms using several widely-used evaluation metrics for multi-label classification. The metrics include Precision ($P@k$), nDCG (nDCG@ k), Propensity Scored precision (PSP@ k), and Propensity Scored nDCG (PSnDCG@ k). These metrics are defined as follows:

$$P@k = \mathbb{E}_{\mathbf{x}} \left[\sum_{i \in Top_k(y)} \frac{1}{k} \cdot \mathbb{P}(y^{(i)} = 1 | \mathbf{x}) \right], \quad (23)$$

$$nDCG@k = \mathbb{E}_{\mathbf{x}} \left[\sum_{i \in Top_k(y)} \frac{\mathbb{P}(y^{(i)} = 1 | \mathbf{x})}{\log(i+1) \cdot \sum_{i=1}^k \frac{1}{\log(i+1)}} \right], \quad (24)$$

$$PSP@k = \mathbb{E}_{\mathbf{x}} \left[\sum_{i \in Top_k(y)} \frac{1}{k} \cdot \frac{\mathbb{P}(y^{(i)} = 1 | \mathbf{x})}{\xi^{(i)}} \right], \quad (25)$$

$$\begin{aligned} &PSnDCG@k \\ &= \mathbb{E}_{\mathbf{x}} \left[\sum_{i \in Top_k(y)} \frac{\mathbb{P}(y^{(i)} = 1 | \mathbf{x})}{\xi^{(i)} \cdot \log(i+1) \cdot \sum_{i=1}^k \frac{1}{\log(i+1)}} \right], \quad (26) \end{aligned}$$

where

$$\begin{aligned} &\mathbb{P}(y_*^{(i)} = 1 | \mathbf{x}) \\ &= \mathbb{P}(y^{(i)} = 1 | \mathbf{x}) \cdot \mathbb{E}_{y^{(-i)} | \mathbf{x}, y^{(i)}=1} \left[\frac{1}{1 + \sum_{j \neq i} y^{(j)}} \right], \quad (27) \end{aligned}$$

$Top_k(y)$ returns the k largest indices of y ranked in descending order, $y^{(-i)}$ denotes the vector of all but the i -th label, and $\xi^{(i)}$

TABLE VII: Experimental results (mean \pm std) on the MLC benchmark datasets measured by PSP@1 (PSnDCG@1). \bullet/\circ indicates whether SLDL is statistically superior/inferior to the comparing methods.

Dataset	SLEEC [38]	DXML [52]	Focal [45]	CB [47]	DB [43]	PACA [31]	FLEM [22]	DELA [21]	CLIF [19]	SLDL (Ours)
cal500	37.64 \pm 1.61	37.48 \pm 1.34	37.54 \pm 1.55	37.56 \pm 1.75	36.65 \pm 1.68	37.79 \pm 1.45	37.75 \pm 1.46	36.67 \pm 1.75	36.58 \pm 1.92	38.31\pm1.20
corel16k-s1	24.64 \pm 0.98	20.66 \pm 0.64	22.55 \pm 0.56	22.53 \pm 0.66	20.73 \pm 0.48	19.55 \pm 1.20	24.17 \pm 0.83	19.66 \pm 0.57	18.81 \pm 0.87	25.10\pm0.91
corel16k-s2	24.15 \pm 0.85	20.09 \pm 0.76	22.57 \pm 0.66	22.44 \pm 0.69	20.53 \pm 1.08	19.31 \pm 1.10	24.04 \pm 0.95	19.52 \pm 0.73	18.53 \pm 0.87	24.66\pm0.78
corel16k-s3	24.28 \pm 0.96	20.64 \pm 0.94	22.16 \pm 1.21	22.25 \pm 1.15	20.26 \pm 1.26	19.53 \pm 1.03	23.51 \pm 0.89	19.39 \pm 0.92	18.59 \pm 1.02	24.81\pm1.05
CUB	58.16 \pm 1.23	55.76 \pm 0.78	56.60 \pm 0.73	56.71 \pm 0.93	57.63 \pm 1.09	58.27 \pm 0.87	54.99 \pm 0.62	58.33\pm1.09	57.25 \pm 0.85	58.10 \pm 0.85
delicious	33.17 \pm 0.54	28.53 \pm 0.54	33.46 \pm 0.62	33.41 \pm 0.59	33.79\pm0.49	32.82 \pm 0.55	33.71 \pm 0.38	33.08 \pm 0.45	31.21 \pm 0.40	33.72 \pm 0.74
eurlex-dc	41.46 \pm 1.34	40.44 \pm 0.71	15.66 \pm 0.88	15.60 \pm 0.89	16.33 \pm 0.95	30.47 \pm 2.36	13.04 \pm 0.84	32.10 \pm 1.16	44.86 \pm 1.14	48.68\pm1.21
eurlex-sm	48.42 \pm 1.11	51.37 \pm 0.82	23.46 \pm 1.08	23.47 \pm 1.08	20.46 \pm 0.85	49.06 \pm 1.61	20.55 \pm 0.94	45.10 \pm 0.94	58.26\pm0.70	57.36 \pm 1.17
espgame	24.70 \pm 0.77	19.75 \pm 0.95	24.14 \pm 1.22	24.29 \pm 1.08	23.94 \pm 1.08	25.79 \pm 0.99	24.81 \pm 1.05	23.90 \pm 0.97	22.53 \pm 0.62	28.06\pm0.80
stackex-chemistry	14.06 \pm 0.84	17.69 \pm 0.90	24.02 \pm 1.22	23.94 \pm 1.26	23.02 \pm 1.14	24.53 \pm 0.93	20.65 \pm 1.24	27.70 \pm 1.28	25.58 \pm 1.19	30.30\pm0.70
stackex-chess	12.61 \pm 2.09	26.55 \pm 2.27	20.25 \pm 1.60	20.89 \pm 2.32	18.86 \pm 1.84	19.96 \pm 2.01	17.57 \pm 1.70	24.00 \pm 2.37	22.79 \pm 2.44	28.65\pm2.87
stackex-coffee	28.75 \pm 8.49	19.85 \pm 6.99	15.46 \pm 8.03	16.71 \pm 7.32	17.45 \pm 9.82	10.01 \pm 4.57	17.47 \pm 9.18	20.00 \pm 6.95	22.05 \pm 9.11	32.92\pm8.27
stackex-cooking	15.12 \pm 0.71	18.46 \pm 5.30	27.06 \pm 0.93	27.15 \pm 0.94	26.26 \pm 1.15	29.57 \pm 1.28	21.51 \pm 0.78	33.93 \pm 0.93	31.86 \pm 0.75	39.06\pm0.80
stackex-cs	15.88 \pm 0.78	24.33 \pm 1.07	28.92 \pm 1.38	28.88 \pm 1.37	30.21 \pm 1.17	30.21 \pm 1.09	25.11 \pm 1.34	34.33 \pm 1.59	31.78 \pm 1.15	34.47\pm1.64
stackex-philosophy	11.06 \pm 1.21	27.21 \pm 1.56	21.29 \pm 1.51	21.26 \pm 1.33	19.74 \pm 1.59	22.19 \pm 2.39	18.81 \pm 1.26	26.97 \pm 1.73	26.27 \pm 1.69	31.50\pm1.68
Avg. Rank	5.53	6.60	6.07	6.00	6.60	5.60	6.33	5.07	5.80	1.33

TABLE VIII: Experimental results (mean \pm std) on the MLC benchmark datasets measured by PSP@5. \bullet/\circ indicates whether SLDL is statistically superior/inferior to the comparing methods.

Dataset	SLEEC [38]	DXML [52]	Focal [45]	CB [47]	DB [43]	PACA [31]	FLEM [22]	DELA [21]	CLIF [19]	SLDL (Ours)
cal500	39.30 \pm 1.83	38.80 \pm 1.99	38.53 \pm 2.04	38.61 \pm 1.94	37.68 \pm 1.41	38.65 \pm 1.88	38.67 \pm 1.68	38.42 \pm 1.67	38.64 \pm 2.58	39.89\pm1.76
corel16k-s1	33.00 \pm 0.89	28.37 \pm 1.07	30.84 \pm 0.53	30.85 \pm 0.53	28.34 \pm 0.72	25.65 \pm 1.13	32.77 \pm 0.54	26.64 \pm 0.54	25.79 \pm 0.84	34.08\pm0.71
corel16k-s2	32.78 \pm 1.16	27.88 \pm 0.88	30.77 \pm 1.09	30.76 \pm 1.13	28.18 \pm 0.85	26.24 \pm 0.86	32.72 \pm 1.14	26.71 \pm 0.85	25.92 \pm 1.17	34.01\pm1.33
corel16k-s3	33.47 \pm 1.01	28.72 \pm 0.99	31.42 \pm 1.02	31.40 \pm 0.93	28.74 \pm 0.99	26.18 \pm 1.29	33.19 \pm 1.17	26.88 \pm 0.89	26.04 \pm 0.90	34.34\pm0.83
CUB	59.88 \pm 0.91	52.67 \pm 0.93	57.29 \pm 0.91	57.44 \pm 1.07	58.92 \pm 0.94	59.39 \pm 1.00	55.03 \pm 0.67	60.32\pm0.92	58.71 \pm 1.14	59.18 \pm 0.78
delicious	34.84 \pm 0.63	28.93 \pm 0.54	34.73 \pm 0.45	34.70 \pm 0.52	34.64 \pm 0.53	34.61 \pm 0.61	35.02 \pm 0.41	34.87 \pm 0.52	32.93 \pm 0.50	35.85\pm0.56
eurlex-dc	60.18 \pm 1.61	60.92 \pm 1.33	22.28 \pm 1.11	22.20 \pm 1.14	23.69 \pm 1.00	44.21 \pm 2.25	19.39 \pm 0.96	48.45 \pm 1.10	62.30 \pm 1.37	64.77\pm1.19
eurlex-sm	65.97 \pm 1.01	68.62 \pm 0.91	35.37 \pm 1.15	35.35 \pm 1.17	36.41 \pm 1.24	62.02 \pm 1.44	31.41 \pm 1.02	58.40 \pm 1.20	72.45 \pm 0.49	73.12\pm0.83
espgame	26.04 \pm 0.41	20.82 \pm 0.53	26.07 \pm 0.53	26.10 \pm 0.58	24.57 \pm 0.56	25.99 \pm 0.65	26.68 \pm 0.50	25.46 \pm 0.57	24.34 \pm 0.44	30.19\pm0.37
stackex-chemistry	23.35 \pm 0.81	27.87 \pm 1.34	38.06 \pm 1.25	37.93 \pm 1.31	36.63 \pm 1.05	36.02 \pm 1.42	32.20 \pm 0.80	40.07 \pm 0.75	37.55 \pm 0.68	41.86\pm0.71
stackex-chess	21.27 \pm 1.95	36.28 \pm 2.99	29.07 \pm 1.90	29.45 \pm 2.17	29.04 \pm 2.03	29.48 \pm 2.50	26.56 \pm 1.96	35.45 \pm 2.13	35.07 \pm 2.37	37.81\pm1.84
stackex-coffee	58.14 \pm 7.81	37.40 \pm 8.15	31.72 \pm 8.67	30.32 \pm 9.49	31.82 \pm 8.21	22.23 \pm 6.44	34.19 \pm 11.45	45.27 \pm 10.29	40.19 \pm 9.85	58.48\pm9.85
stackex-cooking	19.88 \pm 0.61	25.13 \pm 4.76	35.77 \pm 0.78	35.75 \pm 0.80	35.11 \pm 0.90	35.65 \pm 1.65	30.16 \pm 0.85	40.46 \pm 0.83	38.36 \pm 1.18	42.47\pm0.81
stackex-cs	22.94 \pm 0.86	34.82 \pm 1.35	43.14 \pm 1.30	42.99 \pm 1.17	43.02 \pm 1.00	41.78 \pm 1.23	37.51 \pm 0.89	47.13 \pm 1.32	45.10 \pm 1.46	47.44\pm1.33
stackex-philosophy	19.06 \pm 1.03	35.55 \pm 1.49	29.89 \pm 1.20	29.86 \pm 1.07	30.33 \pm 1.52	29.50 \pm 2.29	25.30 \pm 1.08	34.56 \pm 1.27	35.36 \pm 1.93	37.99\pm1.41
Avg. Rank	5.27	6.33	5.73	6.13	6.73	6.93	6.27	4.73	5.67	1.20

is the propensity score for the i -th label which defined in [81]. In this experiment, we utilize P@1 (equal to nDCG@1), P@3, P@5, nDCG@3, nDCG@5, PSP@1 (equal to PSnDCG@1), PSP@5, and PSnDCG@5 to evaluate each algorithm.

C. Performance Comparison

Tables II to IX present the experimental results of different algorithms evaluated using six evaluation metrics. For SLDL, the threshold τ for optimizing the target embedding distributions is set to 0.1, the balancing factor α is set to 1, the embedding dimension \hat{c} and the number of neighbors k are selected through grid search from the set $\{16, 32, \dots, 128\}$ and $\{10, 20, \dots, 100\}$, respectively. We perform ten-fold cross-validation for each algorithm and record the mean values and standard deviations of different methods on each evaluation metric. The two-tailed t-test at 0.05 significance level is conducted, and the best performance on each dataset is denoted in boldface. \bullet/\circ indicates whether SLDL is statistically superior/inferior to the comparing methods. Additionally, the

average rank of each algorithm across all datasets is presented in the last row of each table.

From Tables II to IX, it can be observed that SLDL outperforms existing multi-label classification algorithms in almost all cases. Moreover, SLDL can consistently statistically outperform the state-of-art multi-label classification methods in most cases. These experimental results reveals the effectiveness of the asymmetric-correlational Gaussian embedding approach in SLDL and its ability to improve the classification performance. When considering the average ranks across all fifteen benchmark datasets, SLDL demonstrates competitive performance compared to other algorithms. Especially, SLDL achieves 1st or 2nd in 95.8% cases when compared to these state-of-the-art algorithms. Therefore, SLDL exhibits superior performance over the state-of-the-art algorithms across all evaluation metrics.

To further investigate the relative performance among the comparing algorithms, a statistical test, *Friedman test*, is conducted. Table X reports the Friedman statistics F_F and the corresponding critical value on each evaluation criterion.

TABLE IX: Experimental results (mean \pm std) on the MLC benchmark datasets measured by PSnDCG@5. \bullet / \circ indicates whether SLDL is statistically superior/inferior to the comparing methods.

Dataset	SLEEC [38]	DXML [52]	Focal [45]	CB [47]	DB [43]	PACA [31]	FLEM [22]	DELA [21]	CLIF [19]	SLDL (Ours)
cal500	38.72 \pm 1.50	38.37 \pm 1.58	38.22 \pm 1.73	38.34 \pm 1.87	37.37 \pm 1.44	38.32 \pm 1.60	38.36 \pm 1.50	37.85 \pm 1.56	38.05 \pm 2.30	39.34\pm1.44
corel16k-s1	29.43 \pm 0.81	25.09 \pm 0.82	27.27 \pm 0.40	27.28 \pm 0.38	25.29 \pm 0.51	23.00 \pm 1.11	29.10 \pm 0.51	23.48 \pm 0.53	22.81 \pm 0.86	30.13\pm0.67
corel16k-s2	28.75 \pm 0.95	24.21 \pm 0.61	26.81 \pm 0.82	26.77 \pm 0.82	24.88 \pm 0.74	22.94 \pm 0.81	28.55 \pm 0.93	23.24 \pm 0.69	22.44 \pm 0.93	29.40\pm1.02
corel16k-s3	29.26 \pm 1.01	24.93 \pm 1.02	27.19 \pm 1.00	27.21 \pm 0.91	25.28 \pm 1.05	23.01 \pm 1.19	28.84 \pm 1.02	23.39 \pm 0.78	22.60 \pm 0.87	29.75\pm1.03
CUB	59.52 \pm 0.94	53.35 \pm 0.81	57.13 \pm 0.83	57.28 \pm 0.99	58.66 \pm 0.92	59.17 \pm 0.95	55.07 \pm 0.66	59.89\pm0.92	58.38 \pm 1.01	58.96 \pm 0.79
delicious	34.50 \pm 0.59	28.84 \pm 0.53	34.45 \pm 0.44	34.42 \pm 0.50	34.49 \pm 0.51	34.22 \pm 0.57	34.75 \pm 0.36	34.48 \pm 0.46	32.55 \pm 0.51	35.32\pm0.64
eurlex-dc	53.63 \pm 1.30	53.47 \pm 0.87	20.92 \pm 0.90	20.86 \pm 0.93	22.39 \pm 0.87	39.54 \pm 2.34	18.26 \pm 0.80	42.64 \pm 0.99	56.04 \pm 1.05	59.53\pm0.96
eurlex-sm	58.84 \pm 1.12	61.65 \pm 0.76	28.62 \pm 1.01	28.62 \pm 1.02	29.99 \pm 1.08	56.52 \pm 1.60	25.53 \pm 0.88	52.22 \pm 1.13	67.09 \pm 0.50	67.40\pm0.98
espgame	24.60 \pm 0.41	19.56 \pm 0.57	24.47 \pm 0.76	24.51 \pm 0.74	23.54 \pm 0.77	25.00 \pm 0.66	25.03 \pm 0.65	24.23 \pm 0.65	23.11 \pm 0.49	28.72\pm0.43
stackex-chemistry	19.67 \pm 0.58	23.65 \pm 0.88	32.64 \pm 1.04	32.55 \pm 1.05	31.40 \pm 1.06	31.45 \pm 1.15	27.85 \pm 0.88	35.30 \pm 0.79	32.76 \pm 0.89	37.07\pm0.84
stackex-chess	17.75 \pm 2.02	32.81 \pm 2.92	25.72 \pm 1.77	26.26 \pm 2.37	25.43 \pm 2.13	25.33 \pm 2.00	23.23 \pm 1.78	31.21 \pm 2.11	30.45 \pm 2.07	34.42\pm2.81
stackex-coffee	46.03\pm8.57	29.33 \pm 7.67	25.01 \pm 7.74	25.03 \pm 6.89	25.15 \pm 7.14	16.53 \pm 5.33	26.77 \pm 9.16	34.57 \pm 9.10	31.80 \pm 8.83	45.78 \pm 9.16
stackex-cooking	17.88 \pm 0.38	22.40 \pm 5.03	32.23 \pm 0.69	32.23 \pm 0.75	31.55 \pm 0.90	33.02 \pm 1.56	26.65 \pm 0.68	37.62 \pm 0.69	35.51 \pm 1.00	40.40\pm0.80
stackex-cs	19.49 \pm 0.83	30.07 \pm 0.99	37.28 \pm 1.07	37.18 \pm 0.97	37.78 \pm 0.92	36.67 \pm 0.80	32.15 \pm 0.84	41.77 \pm 1.16	39.55 \pm 1.21	41.85\pm1.75
stackex-philosophy	16.95 \pm 1.04	33.80 \pm 1.21	27.79 \pm 1.16	27.75 \pm 1.08	27.44 \pm 1.20	27.61 \pm 2.15	23.92 \pm 1.03	32.55 \pm 1.40	32.67 \pm 1.49	36.42\pm1.04
Avg. Rank	5.00	6.47	6.07	5.93	6.60	6.67	6.27	4.87	5.73	1.27

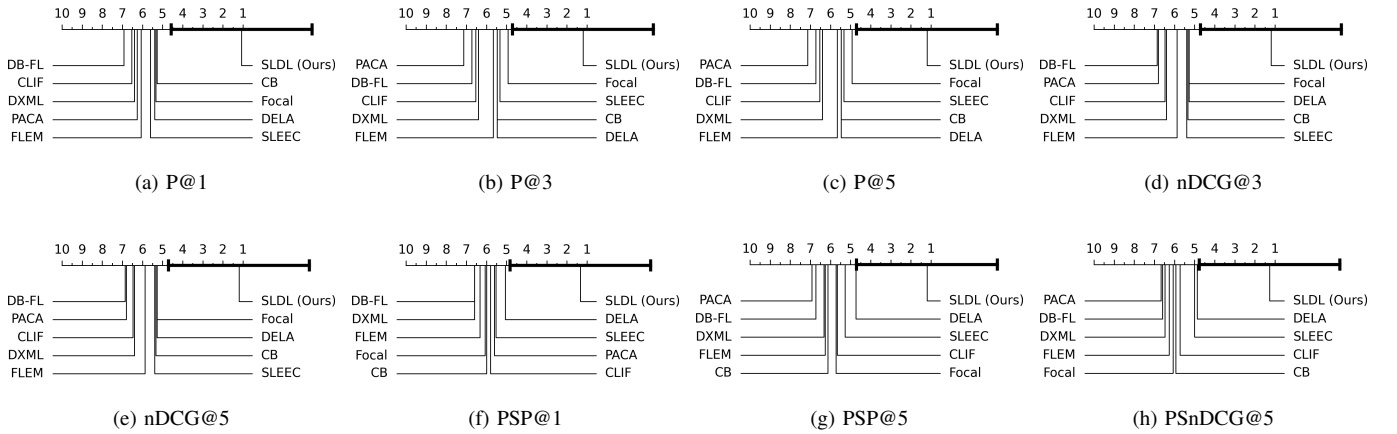


Fig. 3: Comparison of SLDL (control algorithm) against comparing algorithms with the *Nemenyi test*. Algorithms not connected with SLDL in the CD diagram are considered to have a significantly different performance from the control algorithm.

TABLE X: Friedman statistics F_F in terms of each evaluation criterion and the critical value at 0.05 significance level.

Evaluation Criterion	F_F	Critical value
P@1	5.8514	
P@3	6.1696	
P@5	6.0939	
nDCG@3	6.0058	
nDCG@5	5.7533	1.9550
PSP@1	4.9089	
PSP@5	5.9046	
PSnDCG@5	5.5336	

As shown in Table X, the null hypothesis of indistinguishable performance among the compared methods is rejected at a significance level of 0.05 for each evaluation criterion. Subsequently, a *post-hoc Nemenyi test* [82] is applied at a significance level of 0.05 to determine whether the proposed SLDL method achieves competitive performance against the compared algorithms. The critical difference (CD) diagrams

are depicted in Fig. 3. The lines connecting different algorithms in each sub-graph indicate that the corresponding compared algorithm does not exhibit a significant difference from SLDL. From Fig. 3, it can be observed that in all cases, our proposed SLDL method significantly outperforms the existing methods.

D. Analysis of Time Consumption

In this subsection, we compare the training time of different methods. Two representative multi-label classification methods, SLEEC [38] and FLEM [22] are selected for comparison. Among them, SLEEC is a multi-label classification method that is specifically proposed for large-scale output space, and FLEM is a standard LDL-based multi-label classification method. For a fair comparison, all these three methods run on CPU. For SLDL, the embedding dimension \hat{c} is set to 128 and the number of neighbors k is set to 100. The training time of three methods on different datasets are illustrate in Fig. 4. As we can observe in Fig. 4, owing to the leveraging of the

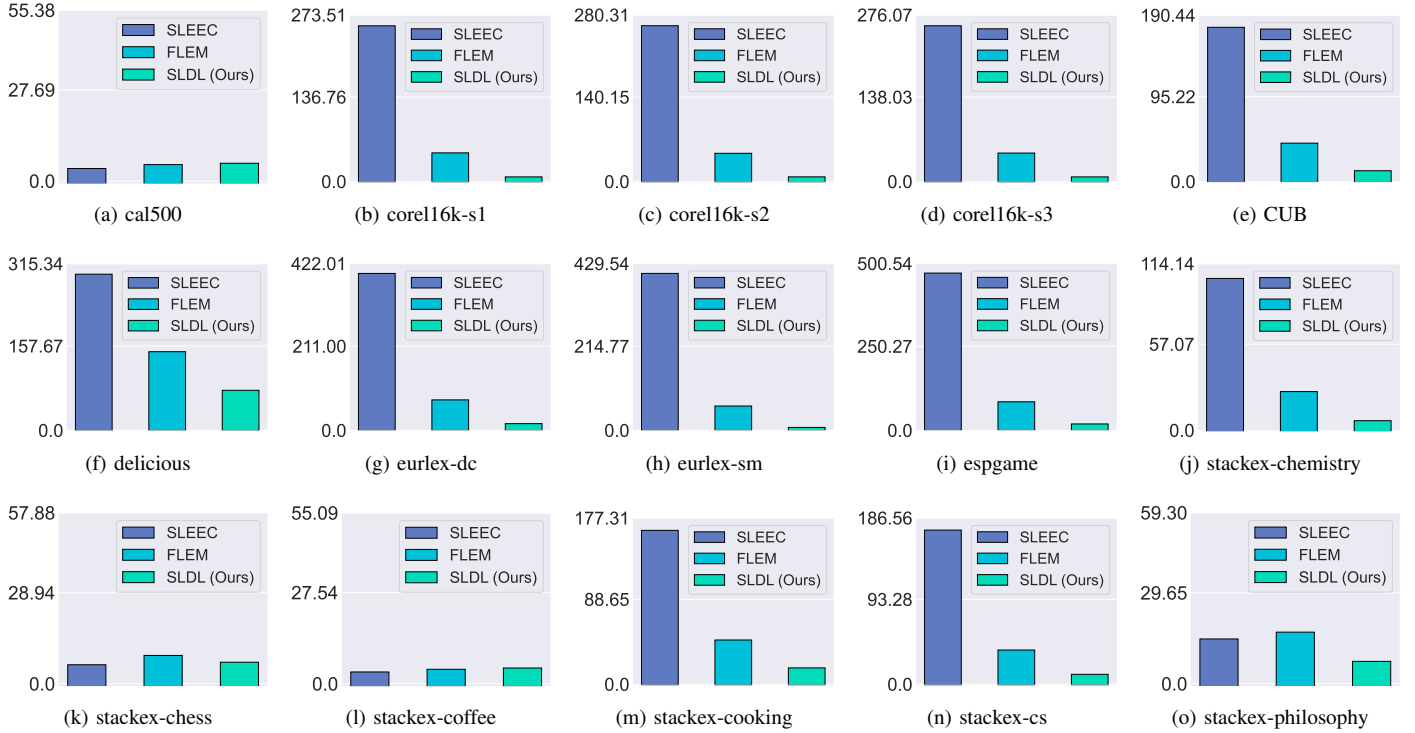


Fig. 4: Training time of SLEEC, FLEM, and SLDL on different datasets. In each subfigure, the x-axis indicates the MLC method, the y-axis indicates the training time (s).

TABLE XI: Comparison of SLDL with different cases on P@5.

Dataset	w/o GE	w/o AC	SLDL (Ours)
cal500	69.32±3.19	68.88±3.26	69.64±3.21
corel16k-s1	23.15±0.51	23.23±0.51	23.40±0.42
corel16k-s2	23.08±0.64	23.31±0.65	23.46±0.65
corel16k-s3	23.31±0.48	23.31±0.58	23.37±0.58
CUB	74.95±0.85	76.25±0.85	76.45±0.83
delicious	56.05±0.72	57.52±0.58	57.64±0.68
eurlex-dc	18.59±0.23	18.63±0.30	18.68±0.30
eurlex-sm	34.13±0.53	34.27±0.57	34.31±0.55
espgame	27.36±0.46	28.15±0.50	28.37±0.40
stackex-chemistry	20.42±0.47	20.63±0.28	21.20±0.37
stackex-chess	22.54±1.30	22.61±1.59	24.24±1.38
stackex-coffee	19.56±2.91	20.17±3.16	22.67±2.97
stackex-cooking	21.61±0.40	21.91±0.33	22.59±0.23
stackex-cs	28.65±0.42	28.55±0.62	28.95±0.47
stackex-philosophy	20.08±0.66	20.66±0.57	22.69±0.56

simple yet effective Gaussian embedding and model training approaches, SLDL can achieve the best results with the least training time in most cases. Specifically, SLDL can achieve 10x or even 100x speedup compared to SLEEC or FLEM on most datasets, which demonstrates the efficiency of SLDL.

E. Ablation Study

1) *Effect of Different Parts*: For a comprehensive understanding of our model, we further design two cases for SLDL to evaluate the effect of the proposed asymmetric-correlational Gaussian embedding approach:

- Case 1 (w/o GE): without learning the Gaussian embedding, i.e., replace latent multivariate Gaussian distributions and Eq.(7) with latent embedding vectors and mean square error loss function.
- Case 2 (w/o AC): without learning the asymmetric correlation among different labels, i.e., replace KL divergence with Jensen–Shannon (JS) divergence.

Table XI tabulates the experimental results of different cases on P@5. From Table XI, we can find that the Gaussian embedding is beneficial to improve the performance. Moreover, the introduction of asymmetric correlation can also promote the performance of the classification model. According to Theorem 1, these results further demonstrates that our embedding approaches are effective and superior. Moreover, the observations further prove the validity of the proposed asymmetric-correlational Gaussian embedding approach.

2) *Effect of Hyperparameters \hat{c} and k* : In this subsection, we explore the effect of hyperparameters \hat{c} and k . We compare the performances of SLDL with different values of \hat{c} and k on the fifteen datasets measured by P@5. Figs. 5 and 6 illustrates the performances of SLDL with different values of \hat{c} and k . From these curves, we can find that: 1) overall, SLDL has stable performances with a wide range of hyperparameter values on all fifteen datasets; 2) the optimum performances of the model can be obtained when the value of \hat{c} is between 64 and 96; 3) appropriate values of k can bring slight performance gains on some datasets. These findings further demonstrate the robustness of the proposed SLDL.

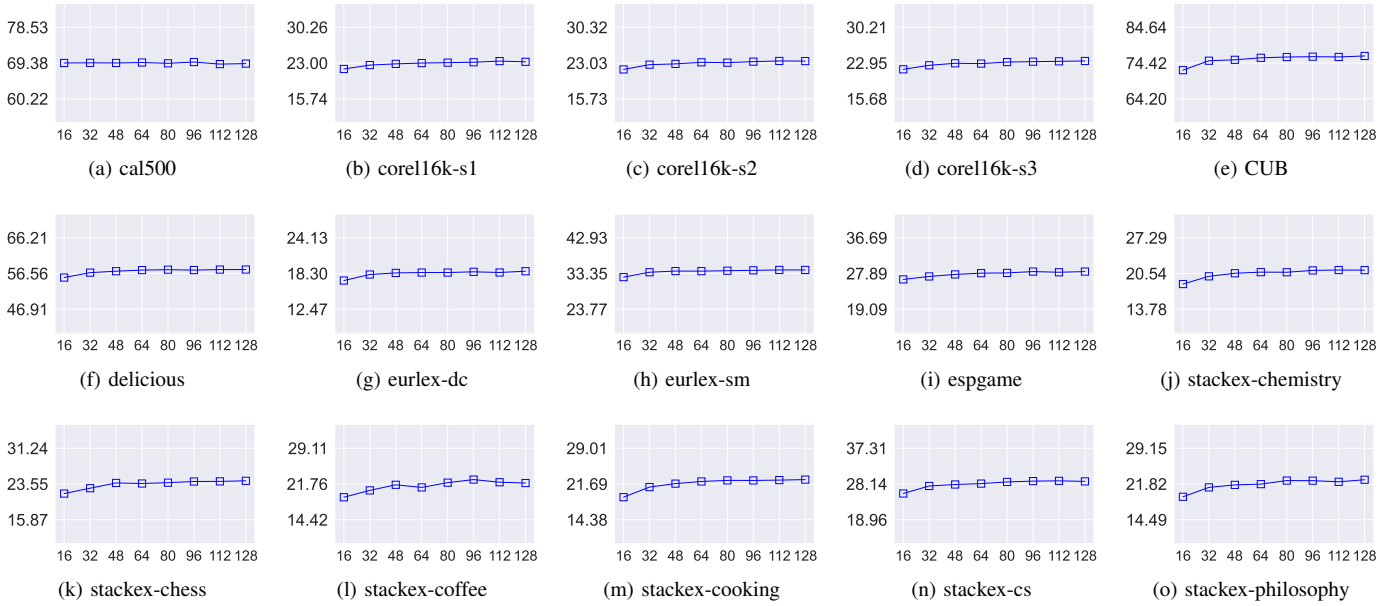


Fig. 5: Effects of \hat{c} on P@5. In each subfigure, the x-axis indicates the value of \hat{c} , the y-axis indicates the value of P@1.

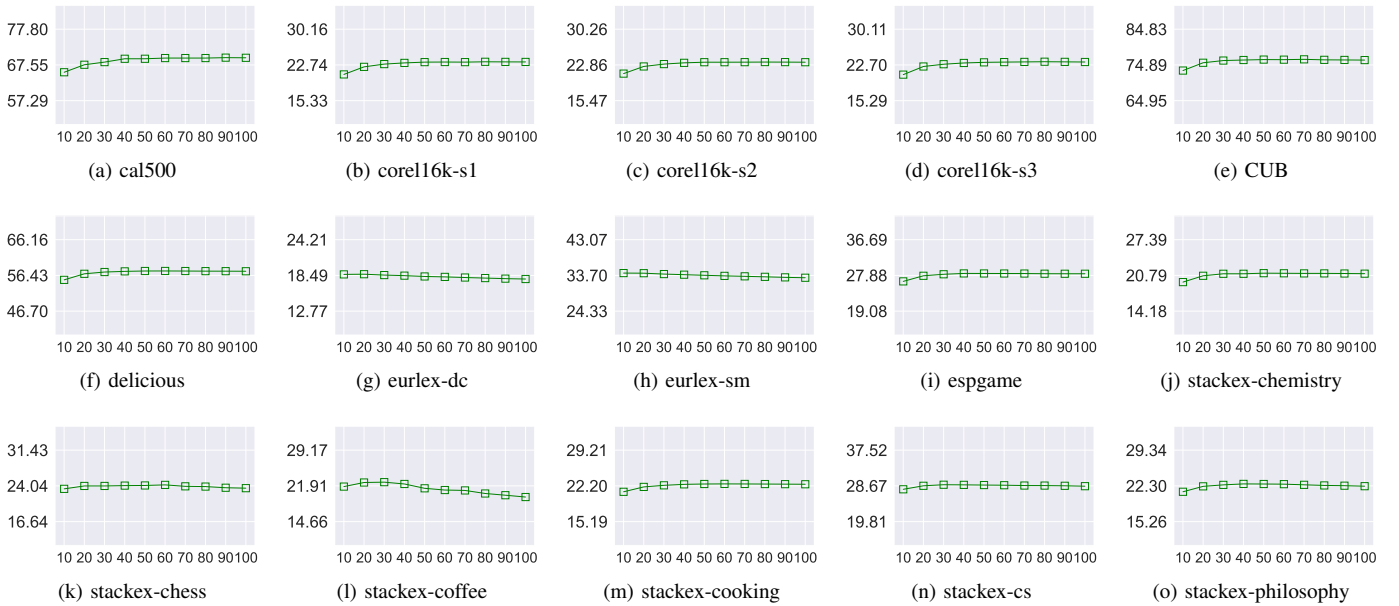


Fig. 6: Effects of k on P@5. In each subfigure, the x-axis indicates the value of k , the y-axis indicates the value of P@5.

V. CONCLUSION

In this paper, a novel label distribution learning approach named SLDL is proposed, which can effectively explore and leverage the asymmetric correlation of different labels in multi-label classification and be well resilient to large-scale output space multi-label classification problems. SLDL can learn the distribution representation of different labels in the latent embedding space to extract the asymmetric correlation among different labels and ameliorate the scalability of model. It first transforms labels into continuous distributions within

a low-dimensional latent space, employing an asymmetric metric to establish correlations between different labels. Subsequently, it learns a mapping from the feature space to the latent space, where computational complexity is no longer tied to the number of labels. Finally, SLDL utilizes a nearest neighbor-based strategy to decode the latent representations and generate the ultimate predictions. The effectiveness of SLDL is proved by both theoretical analysis and experimental results. In future work, we will further explore the theory of SLDL and promote the versatility of SLDL.

REFERENCES

- [1] J. Chu, H. Wang, J. Liu, Z. Gong, and T. Li, "Unsupervised feature learning architecture with multi-clustering integration RBM," in *Proceedings of the 39th IEEE International Conference on Data Engineering*, 2023, pp. 3811–3812.
- [2] R. Guan, H. Zhang, Y. Liang, F. Giunchiglia, L. Huang, and X. Feng, "Deep feature-based text clustering and its explanation," in *Proceedings of the 39th IEEE International Conference on Data Engineering*, 2023, pp. 3871–3872.
- [3] J. Song and B. Moon, "Decoupled instance-label extreme multi-label classification with skew coordinate feature space," in *Proceedings of the 37th IEEE International Conference on Data Engineering*, 2021, pp. 1919–1924.
- [4] X. Geng, "Label distribution learning," *IEEE Transactions on Knowledge and Data Engineering*, vol. 28, no. 7, pp. 1734–1748, 2016.
- [5] M. Zhang and Z. Zhou, "A review on multi-label learning algorithms," *IEEE Trans. Knowl. Data Eng.*, vol. 26, no. 8, pp. 1819–1837, 2014.
- [6] W. Liu, H. Wang, X. Shen, and I. W. Tsang, "The emerging trends of multi-label learning," *IEEE Trans. Pattern Anal. Mach. Intell.*, vol. 44, no. 11, pp. 7955–7974, 2022.
- [7] Y. An, H. Xue, X. Zhao, and J. Wang, "From instance to metric calibration: A unified framework for open-world few-shot learning," *IEEE Trans. Pattern Anal. Mach. Intell.*, vol. 45, no. 8, pp. 9757–9773, 2023.
- [8] Y. An, H. Xue, X. Zhao, and L. Zhang, "Conditional self-supervised learning for few-shot classification," in *Proceedings of the 30th International Joint Conference on Artificial Intelligence*, 2021, pp. 2140–2146.
- [9] Y. An, X. Zhao, and H. Xue, "Learning to learn from corrupted data for few-shot learning," in *Proceedings of the 32nd International Joint Conference on Artificial Intelligence*, 2023, pp. 3423–3431.
- [10] D. Zong and S. Sun, "BGNN-XML: bilateral graph neural networks for extreme multi-label text classification," *IEEE Trans. Knowl. Data Eng.*, vol. 35, no. 7, pp. 6698–6709, 2023.
- [11] J. Zhang, J. Ren, Q. Zhang, J. Liu, and X. Jiang, "Spatial context-aware object-attentional network for multi-label image classification," *IEEE Trans. Image Process.*, vol. 32, pp. 3000–3012, 2023.
- [12] H. Lo, J. Wang, H. Wang, and S. Lin, "Cost-sensitive multi-label learning for audio tag annotation and retrieval," *IEEE Trans. Multim.*, vol. 13, no. 3, pp. 518–529, 2011.
- [13] Z. Gao, P. Qiao, and Y. Dou, "HAAN: human action aware network for multi-label temporal action detection," in *Proceedings of the 31st ACM International Conference on Multimedia*, 2023, pp. 5059–5069.
- [14] H. Wang, Z. Li, J. Huang, P. Hui, W. Liu, T. Hu, and G. Chen, "Collaboration based multi-label propagation for fraud detection," in *Proceedings of the 29th International Joint Conference on Artificial Intelligence*, 2020, pp. 2477–2483.
- [15] J. Li, X. Zhu, and J. Wang, "Adaboost.c2: Boosting classifiers chains for multi-label classification," in *Proceedings of the 37th AAAI Conference on Artificial Intelligence*, 2023, pp. 8580–8587.
- [16] W. Gerych, T. Hartvigsen, L. Buquicchio, E. Agu, and E. A. Rundensteiner, "Recurrent bayesian classifier chains for exact multi-label classification," in *Advances in Neural Information Processing Systems 34*, 2021, pp. 15981–15992.
- [17] J. Read, B. Pfahringer, G. Holmes, and E. Frank, "Classifier chains for multi-label classification," *Mach. Learn.*, vol. 85, no. 3, pp. 333–359, 2011.
- [18] P. Yang, X. Sun, W. Li, S. Ma, W. Wu, and H. Wang, "SGM: Sequence generation model for multi-label classification," in *Proceedings of the 27th International Conference on Computational Linguistics*, 2018, pp. 3915–3926.
- [19] J. Hang and M. Zhang, "Collaborative learning of label semantics and deep label-specific features for multi-label classification," *IEEE Trans. Pattern Anal. Mach. Intell.*, vol. 44, no. 12, pp. 9860–9871, 2022.
- [20] C. Yeh, W. Wu, W. Ko, and Y. F. Wang, "Learning deep latent space for multi-label classification," in *Proceedings of the 31st AAAI Conference on Artificial Intelligence*, 2017, pp. 2838–2844.
- [21] J. Hang and M. Zhang, "Dual perspective of label-specific feature learning for multi-label classification," in *Proceedings of the 39th International Conference on Machine Learning*, vol. 162, 2022, pp. 8375–8386.
- [22] X. Zhao, Y. An, N. Xu, and X. Geng, "Fusion label enhancement for multi-label learning," in *Proceedings of the 31st International Joint Conference on Artificial Intelligence*, 2022, pp. 3773–3779.
- [23] R. Shao, N. Xu, and X. Geng, "Multi-label learning with label enhancement," in *Proceedings of the 2018 IEEE International Conference on Data Mining*, 2018, pp. 437–446.
- [24] N. Xu, C. Qiao, J. Lv, X. Geng, and M. Zhang, "One positive label is sufficient: Single-positive multi-label learning with label enhancement," in *Advances in Neural Information Processing Systems 35*, 2022.
- [25] X. Su, Z. You, D. Huang, L. Wang, L. Wong, B. Ji, and B. Zhao, "Biomedical knowledge graph embedding with capsule network for multi-label drug-drug interaction prediction," *IEEE Trans. Knowl. Data Eng.*, vol. 35, no. 6, pp. 5640–5651, 2023.
- [26] G. Xun, K. Jha, J. Sun, and A. Zhang, "Correlation networks for extreme multi-label text classification," in *Proceedings of the 26th ACM SIGKDD International Conference on Knowledge Discovery and Data Mining*, 2020, pp. 1074–1082.
- [27] F. Wang, S. Mizrahi, M. Beladev, G. Nadav, G. Amsalem, K. L. Assaraf, and H. H. Boker, "Mumic - multimodal embedding for multi-label image classification with tempered sigmoid," in *Proceedings of the 37th AAAI Conference on Artificial Intelligence*, 2023, pp. 15603–15611.
- [28] S. Huang, Y. Yu, and Z. Zhou, "Multi-label hypothesis reuse," in *Proceedings of the 18th ACM SIGKDD International Conference on Knowledge Discovery and Data Mining*, 2012, pp. 525–533.
- [29] J. Bao, Y. Wang, and Y. Cheng, "Asymmetry label correlation for multi-label learning," *Appl. Intell.*, vol. 52, no. 6, pp. 6093–6105, 2022.
- [30] X. Zhao, Y. An, N. Xu, and X. Geng, "Variational continuous label distribution learning for multi-label text classification," *IEEE Transactions on Knowledge and Data Engineering*, 2023.
- [31] J. Hang, M. Zhang, Y. Feng, and X. Song, "End-to-end probabilistic label-specific feature learning for multi-label classification," in *Proceedings of the 36th AAAI Conference on Artificial Intelligence*, 2022, pp. 6847–6855.
- [32] M. R. Boutell, J. Luo, X. Shen, and C. M. Brown, "Learning multi-label scene classification," *Pattern Recognit.*, pp. 1757–1771, 2004.
- [33] M. Zhang, Y. Li, X. Liu, and X. Geng, "Binary relevance for multi-label learning: an overview," *Frontiers Comput. Sci.*, vol. 12, no. 2, pp. 191–202, 2018.
- [34] S. Khandagale, H. Xiao, and R. Babbar, "Bonsai: diverse and shallow trees for extreme multi-label classification," *Mach. Learn.*, vol. 109, no. 11, pp. 2099–2119, 2020.
- [35] H. Jain, V. Balasubramanian, B. Chunduri, and M. Varma, "Slice: Scalable linear extreme classifiers trained on 100 million labels for related searches," in *Proceedings of the 12nd ACM International Conference on Web Search and Data Mining*, 2019, pp. 528–536.
- [36] A. Elisseeff and J. Weston, "A kernel method for multi-labelled classification," in *Advances in Neural Information Processing Systems 14*, 2001, pp. 681–687.
- [37] J. Fürnkranz, E. Hüllermeier, E. L. Mencia, and K. Brinker, "Multilabel classification via calibrated label ranking," *Mach. Learn.*, pp. 133–153, 2008.
- [38] K. Bhatia, H. Jain, P. Kar, M. Varma, and P. Jain, "Sparse local embeddings for extreme multi-label classification," in *Advances in Neural Information Processing Systems 28*, 2015, pp. 730–738.
- [39] Y. Tagami, "Annexml: Approximate nearest neighbor search for extreme multi-label classification," in *Proceedings of the 23rd ACM SIGKDD International Conference on Knowledge Discovery and Data Mining*, 2017, pp. 455–464.
- [40] B. Wang, L. Chen, W. Sun, K. Qin, K. Li, and H. Zhou, "Ranking-based autoencoder for extreme multi-label classification," in *Proceedings of the 2019 Conference of the North American Chapter of the Association for Computational Linguistics: Human Language Technologies*, 2019, pp. 2820–2830.
- [41] C. Guo, A. Mousavi, X. Wu, D. N. Holtmann-Rice, S. Kale, S. J. Reddi, and S. Kumar, "Breaking the glass ceiling for embedding-based classifiers for large output spaces," in *Advances in Neural Information Processing Systems 32*, 2019, pp. 4944–4954.
- [42] V. Gupta, R. Wadbude, N. Natarajan, H. Karnick, P. Jain, and P. Rai, "Distributional semantics meets multi-label learning," in *Proceedings of the 33rd AAAI Conference on Artificial Intelligence*, 2019, pp. 3747–3754.
- [43] T. Wu, Q. Huang, Z. Liu, Y. Wang, and D. Lin, "Distribution-balanced loss for multi-label classification in long-tailed datasets," in *Proceedings of the European Conference on Computer Vision*, 2020, pp. 162–178.
- [44] T. Ridnik, E. B. Baruch, N. Zamir, A. Noy, I. Friedman, M. Protter, and L. Zelnik-Manor, "Asymmetric loss for multi-label classification," in

- Proceedings of the IEEE International Conference on Computer Vision*, 2021, pp. 82–91.
- [45] T. Lin, P. Goyal, R. B. Girshick, K. He, and P. Dollár, “Focal loss for dense object detection,” in *Proceedings of the IEEE International Conference on Computer Vision*, 2017, pp. 2999–3007.
- [46] Y. Huang, B. Giledereli, A. Köksal, A. Özgür, and E. Ozkirimli, “Balancing methods for multi-label text classification with long-tailed class distribution,” in *Proceedings of the 2021 Conference on Empirical Methods in Natural Language Processing*, 2021, pp. 8153–8161.
- [47] Y. Cui, M. Jia, T. Lin, Y. Song, and S. J. Belongie, “Class-balanced loss based on effective number of samples,” in *Proceedings of the IEEE Conference on Computer Vision and Pattern Recognition*, 2019, pp. 9268–9277.
- [48] N. Zhang, X. Chen, X. Xie, S. Deng, C. Tan, M. Chen, F. Huang, L. Si, and H. Chen, “Document-level relation extraction as semantic segmentation,” in *Proceedings of the 30th International Joint Conference on Artificial Intelligence*, 2021, pp. 3999–4006.
- [49] I. E. Yen, X. Huang, P. Ravikumar, K. Zhong, and I. S. Dhillon, “Pd-sparse : A primal and dual sparse approach to extreme multiclass and multilabel classification,” in *Proceedings of the 33rd International Conference on Machine Learning*, vol. 48, 2016, pp. 3069–3077.
- [50] R. Babbar and B. Schölkopf, “Dismec: Distributed sparse machines for extreme multi-label classification,” in *Proceedings of the 10th ACM International Conference on Web Search and Data Mining*, 2017, pp. 721–729.
- [51] Y. Prabhu and M. Varma, “Fastxml: a fast, accurate and stable tree-classifier for extreme multi-label learning,” in *Proceedings of the 20th ACM SIGKDD International Conference on Knowledge Discovery and Data Mining*, 2014, pp. 263–272.
- [52] W. Zhang, J. Yan, X. Wang, and H. Zha, “Deep extreme multi-label learning,” in *Proceedings of the 2018 International Conference on Multimedia Retrieval*, 2018, pp. 100–107.
- [53] J. Liu, W. Chang, Y. Wu, and Y. Yang, “Deep learning for extreme multi-label text classification,” in *Proceedings of the 40th International ACM SIGIR Conference on Research and Development in Information Retrieval*, 2017, pp. 115–124.
- [54] R. You, Z. Zhang, Z. Wang, S. Dai, H. Mamitsuka, and S. Zhu, “Attentionxml: Label tree-based attention-aware deep model for high-performance extreme multi-label text classification,” in *Advances in Neural Information Processing Systems 32*, 2019, pp. 5812–5822.
- [55] X. Zhao, Y. An, N. Xu, J. Wang, and X. Geng, “Imbalanced label distribution learning,” in *Proceedings of the 37th AAAI Conference on Artificial Intelligence*, 2023, pp. 11 336–11 344.
- [56] X. Zhao, L. Qi, Y. An, and X. Geng, “Generalizable label distribution learning,” in *Proceedings of the 31st ACM International Conference on Multimedia*, 2023, pp. 8932–8941.
- [57] K. Su and X. Geng, “Soft facial landmark detection by label distribution learning,” in *Proceedings of the 33rd AAAI Conference on Artificial Intelligence*, 2019, pp. 5008–5015.
- [58] B. Gao, H. Zhou, J. Wu, and X. Geng, “Age estimation using expectation of label distribution learning,” in *Proceedings of the 27th International Joint Conference on Artificial Intelligence*, 2018, pp. 712–718.
- [59] X. Geng and Y. Xia, “Head pose estimation based on multivariate label distribution,” in *Proceedings of the IEEE Conference on Computer Vision and Pattern Recognition*, 2014, pp. 1837–1842.
- [60] Z. Huo and X. Geng, “Ordinal zero-shot learning,” in *Proceedings of the 26th International Joint Conference on Artificial Intelligence*, 2017, pp. 1916–1922.
- [61] D. Zhou, X. Zhang, Y. Zhou, Q. Zhao, and X. Geng, “Emotion distribution learning from texts,” in *Proceedings of the 2016 Conference on Empirical Methods in Natural Language Processing*, 2016, pp. 638–647.
- [62] A. L. Berger, S. A. Della Pietra, and V. J. Della Pietra, “A maximum entropy approach to natural language processing,” *Computational Linguistics*, vol. 22, no. 1, pp. 39–71, 1996.
- [63] S. D. Pietra, V. J. D. Pietra, and J. D. Lafferty, “Inducing features of random fields,” *IEEE Trans. Pattern Anal. Mach. Intell.*, vol. 19, no. 4, pp. 380–393, 1997.
- [64] X. Yang, X. Geng, and D. Zhou, “Sparsity conditional energy label distribution learning for age estimation,” in *Proceedings of the 25th International Joint Conference on Artificial Intelligence*, 2016, pp. 2259–2265.
- [65] X. Geng and P. Hou, “Pre-release prediction of crowd opinion on movies by label distribution learning,” in *Proceedings of the 24th International Joint Conference on Artificial Intelligence*, 2015, pp. 3511–3517.
- [66] W. Shen, K. Zhao, Y. Guo, and A. L. Yuille, “Label distribution learning forests,” in *Advances in Neural Information Processing Systems 30*, 2017, pp. 834–843.
- [67] B. Gao, C. Xing, C. Xie, J. Wu, and X. Geng, “Deep label distribution learning with label ambiguity,” *IEEE Transactions on Image Processing*, vol. 26, no. 6, pp. 2825–2838, 2017.
- [68] Y. Zhou, H. Xue, and X. Geng, “Emotion distribution recognition from facial expressions,” in *Proceedings of the 23rd ACM International Conference on Multimedia*, 2015, pp. 1247–1250.
- [69] X. Jia, W. Li, J. Liu, and Y. Zhang, “Label distribution learning by exploiting label correlations,” in *Proceedings of the 32nd AAAI Conference on Artificial Intelligence*, 2018, pp. 3310–3317.
- [70] M. Xu and Z. Zhou, “Incomplete label distribution learning,” in *Proceedings of the 26th International Joint Conference on Artificial Intelligence*, 2017, pp. 3175–3181.
- [71] P. Zhao and Z. Zhou, “Label distribution learning by optimal transport,” in *Proceedings of the 32nd AAAI Conference on Artificial Intelligence*, 2018, pp. 4506–4513.
- [72] T. Ren, X. Jia, W. Li, L. Chen, and Z. Li, “Label distribution learning with label-specific features,” in *Proceedings of the 28th International Joint Conference on Artificial Intelligence*, 2019, pp. 3318–3324.
- [73] X. Jia, X. Zheng, W. Li, C. Zhang, and Z. Li, “Facial emotion distribution learning by exploiting low-rank label correlations locally,” in *Proceedings of the IEEE Conference on Computer Vision and Pattern Recognition*, 2019, pp. 9841–9850.
- [74] X. Zheng, X. Jia, and W. Li, “Label distribution learning by exploiting sample correlations locally,” in *Proceedings of the 32nd AAAI Conference on Artificial Intelligence*, 2018, pp. 4556–4563.
- [75] X. Jia, Z. Li, X. Zheng, W. Li, and S. Huang, “Label distribution learning with label correlations on local samples,” *IEEE Trans. Knowl. Data Eng.*, vol. 33, no. 4, pp. 1619–1631, 2021.
- [76] T. Ren, X. Jia, W. Li, and S. Zhao, “Label distribution learning with label correlations via low-rank approximation,” in *Proceedings of the 28th International Joint Conference on Artificial Intelligence*, 2019, pp. 3325–3331.
- [77] X. Zhao, Y. An, N. Xu, and X. Geng, “Continuous label distribution learning,” *Pattern Recognit.*, vol. 133, p. 109056, 2023.
- [78] R. H. Byrd, P. Lu, J. Nocedal, and C. Zhu, “A limited memory algorithm for bound constrained optimization,” *SIAM J. Sci. Comput.*, vol. 16, no. 5, pp. 1190–1208, 1995.
- [79] N. Jorge and J. W. Stephen, *Numerical optimization*. Springer, 2006.
- [80] K. Huang and H. Lin, “Cost-sensitive label embedding for multi-label classification,” *Mach. Learn.*, vol. 106, no. 9-10, pp. 1725–1746, 2017.
- [81] H. Jain, Y. Prabhu, and M. Varma, “Extreme multi-label loss functions for recommendation, tagging, ranking & other missing label applications,” in *Proceedings of the 22nd ACM SIGKDD International Conference on Knowledge Discovery and Data Mining*, 2016, pp. 935–944.
- [82] J. Demsar, “Statistical comparisons of classifiers over multiple data sets,” *J. Mach. Learn. Res.*, vol. 7, pp. 1–30, 2006.